Front. Optoelectron. 2019, 12(3): 229–248
https://doi.org/10.1007/s12200-019-0901-x

REVIEW ARTICIE

Review on partially coherent vortex beams

Jun ZENG[1], Rong LIN[2,3], Xianlong LIU[2], Chengliang ZHAO[1], Yangjian CAI (✉)[1,2]

1 School of Physical Science and Technology, Soochow University, Suzhou 215006, China
2 Shandong Provincial Engineering and Technical Center of Light Manipulations & Shandong Provincial Key Laboratory of Optics and Photonic Device, School of Physics and Electronics, Shandong Normal University, Jinan 250014, China
3 College of Physics and Electronic Engineering, Heze University, Heze 274015, China

Abstract Ever since vortex beams were proposed, they are known for owning phase singularity and carrying orbital angular momentum (OAM). In the past decades, coherent optics developed rapidly. Vortex beams have been extended from fully coherent light to partially coherent light, from scalar light to vector light, from integral topological charge (TC) to fractional TC. Partially coherent vortex beams have attracted tremendous interest due to their hidden correlation singularity and unique propagation properties (e.g., beam shaping, beam rotation and self-reconstruction). Based on the sufficient condition for devising a genuine correlation function of partially coherent beam, partially coherent vortex beams with nonconventional correlation functions (i.e., non-Gaussian correlated Schell-model functions) were introduced recently. This timely review summarizes basic concepts, theoretical models, generation and propagation of partially coherent vortex beams.

Keywords partially coherent vortex beam, phase singularity, correlation singularity, topological charge (TC), coherence length, correlation function

1 Introduction

In 1974, Nye and Berry introduced a new kind fundamental property of light field, namely wave front dislocation (or phase defect) [1], which includes edge dislocation, screw dislocation and mixed edge-screw dislocation. The screw dislocation, the most common wave front dislocation will introduce a phase singularity at the center of the beam with zero amplitude and indefinite phase, and phase singularity of the wave function ψ appears at the point where its modulus vanishes, i.e., when $\mathrm{Re}(\psi) = \mathrm{Im}(\psi) = 0$. Following this pioneering work, these dislocations, or phase singularities, become a separate area of investigation in modern optics, named singular optics [2]. The main object of singular optics is optical vortex (screw dislocation). As pointed out by Allen in 1992, a vortex beam with helical phase front, described by a phase term $\exp(il\theta)$, carries an orbital angular momentum (OAM) of $l\hbar$ per photon, where l is the topological charge (TC), θ is the azimuthal angle, and $\hbar$ is reduced Planck constant. Because this TC is quantized, it remains constant under small deformations. As pointed out by Gbur and Tyson, the TC of the vortex beams propagating through atmospheric turbulence is a robust quantity that could be used as an information carrier in optical communications [3]. In addition, because of conservation of TC of optical vortices, an unusual optical phenomenon (namely, existence of bound optical states in the radiation continuum) has been found in the radiation continuum [4]. Increasing attention has been paid to optical vortices (e.g., Gaussian-like beam [5], Bessel beam [6–8], anomalous vortex beam [9] and perfect vortex beam [10,11]) due to their important applications in free-space optical communications [12,13], optical manipulation [14–18], quantum information processing [19–21], optical measurements [22,23], super-resolution imaging [24,25] and so on. To introduce TC or OAM to light beam, several methods have been exploited [26–37]. Quantitative measurement of TC or OAM state of vortex beams is important in exploiting their applications. Many methods, such as Shack Hartmann wave front sensor [38], interference [39,40], diffraction [41–43], scattering [44], Fourier patterns of the intensity [45], mode transformation [46], OAM density [47], rotational Doppler effect [48], have been proposed for this purpose. Above mentioned literatures are limited to vortex beams with integral TC, and in fact, the value of TC can be non-integral (i.e.,

Received January 3, 2019; accepted January 28, 2019

E-mail: yangjiancai@suda.edu.cn

Invited, Wuhan Optoelectronics Forum (WHOF) 137

fractional TC). The vortex beam with fractional TC (i.e., fractional vortex beam), which possesses a radial opening in the annular intensity ring, was first observed by Basistiy et al. [49]. Later, many studies on fractional vortex beams have been reported [50–63].

In addition to intensity and phase, the beam itself has another important controllable parameter called coherence [64], which includes temporal coherence and spatial coherence. Temporal coherence is closely related to the monochromatism of a beam, while spatial coherence is closely related to the directivity of a beam. In this paper, we restrict our focus on spatial coherence. Laser beam is known for its high spatial coherence and is usually treated as a fully coherent beam. It is generally believed that with the decrease of spatial coherence, the divergence of the beam increases, which is not conducive to practical applications. Since 1970s, numerous efforts have been paid to the coherence of light beam [65–72]. Light beam with low spatial coherence, so-called partially coherent beam, exhibits some unique optical properties and superiority in many applications. For example, decreasing the spatial coherence of a light beam can increase the signal-noise ratio and reduce the bit-error rate in free-space optical communications [73,74]. Partially coherent beams can effectively overcome speckle in laser nuclear fusion [75], and such beam can be used to reduce noise in photograph [76] and to realize classic ghost interference [77]. In addition, partially coherent beams have advantages over coherent beams in particle trapping [78], atom cooling [79], second-harmonic generation [80,81], optical scattering [82,83] and laser scanning [84].

The research scope of singular optics has been extended from fully coherent vortex beam to partially coherent vortex beam since Gori et al. proposed the partially coherent sources with helicoidal modes [85]. When a light beam is partially coherent, its random fluctuations tend to move its singular points, leaving no zeros in the average intensity [86]. It was demonstrated that the zeros disappear as the coherence of the light beam decreases [87,88]. However, partially coherent vortex beams possess singularities in some hidden form, a good candidate for such hidden vortices is the singularities of two-point correlation functions described, so-called coherence vortices [89]. As pointed out by Gbur and Visser, coherence vortices are a generic feature of partially coherent light field [89]. Based on these basic studies, partially coherent vortex beams with conventional correlation functions (i.e., Gaussian correlated Schell-model functions) attract more and more attention [90–105].

Since Gori's pioneering work about establishment of the sufficient condition for devising a genuine correlation function of a scalar partially coherent beam [106] and a genuine cross-spectral density matrix of an electromagnetic stochastic beam [107], various partially coherent beams with nonconventional correlation functions (i.e., non-Gaussian correlated Schell-model functions) were introduced [108–111]. The research scopes of partially coherent vortex beams have been extended to partially coherent vortex beams with nonconventional correlation functions [112–114] and vector cases [115–117], respectively. Modulating spatial coherence, topological charge and degree of polarization of a partially coherent vortex beam provides a novel way for shaping the focused intensity distribution (i.e., dark-hollow, flat-topped or Gaussian beam spots) [94,115,117], which is useful for optical trapping [118]. Partially coherent vortex beam (i.e., Gaussian–Schell model vortex beam) has appreciably smaller scintillation than a partially coherent beam without vortex phase (i.e., Gaussian–Schell model beam) [119], which will be useful in free-space optical communications. In addition, the complex degree of coherence of a partially coherent vortex beam exhibits self-reconstruction ability on propagation [102], which can be used for measuring the topological charge of partially coherent vortex beam and information encryption and decryption. Recently, a new kind of partially coherent vortex (PCV) beam with fractional topological charge [i.e., partially coherent fractional vortex (PCFV) beam] was introduced [120]. The opening gap of the intensity pattern and the rotation property of the PCFV beam spot disappear gradually on propagation, while the cross-spectral density (CSD) distribution becomes more symmetric and more recognizable with the decrease of spatial coherence [120]. Due to their interesting properties and potential applications, generation and measurement of partially coherent vortex beams have been explored extensively [113,115,121–127]. In this paper, we introduce recent developments on partially coherent vortex beams including basic concepts, theoretical models, generation and propagation.

2 Basic concept of singularity optics

The research subject of singular optics are optical vortex, wave front dislocation and wave front topological structure in the neighborhood of phase singularity. The research scope of singular optics has been extended from fully coherent light to partially coherent light, from scalar light wave field to vector light wave field, from theoretical research and computational simulation to experimental and applied researches. In this section, we give a brief introduction to the basic concept of singularity optics.

2.1 Phase singularities

According to the electromagnetic field theory, the complex electric field of any point $\boldsymbol{r}$ can be expressed as

$$E(\boldsymbol{r}) = E_{\mathrm{R}}(\boldsymbol{r}) + \mathrm{i}E_{\mathrm{I}}(\boldsymbol{r}) = A(\boldsymbol{r})\exp[\mathrm{i}\varphi(\boldsymbol{r})], \tag{1}$$

where $E_{\mathrm{R}}(\boldsymbol{r})$ and $E_{\mathrm{I}}(\boldsymbol{r})$ are real and imaginary parts of complex electric field, $A(\boldsymbol{r})$ is the amplitude, $\varphi(\boldsymbol{r}) = \arctan[E_{\mathrm{R}}(\boldsymbol{r})/E_{\mathrm{I}}(\boldsymbol{r})]$ denotes the phase which is between $-\pi$ and

π. Consider that $E(\boldsymbol{r})$ in the space-time domain is a single value function, and the distribution of $E(\boldsymbol{r})$ displays smooth transitions. Now, as it goes around a loop C, the magnitude of the change in phase φ must be integral multiple of 2π, namely $2\pi l$ (l is an integer). From a mathematical point of view, let's assume that l ($l \neq 0$) is fixed, by compressing loop C indefinitely into a small enough area, one sees that the change rate of the phase φ is approaching infinity, that is, the loop surrounds around a singularity. Based on the smoothness of the field distribution function, the position of the phase singularity is the place where the electric field intensity is zero, i.e., $E_{\mathrm{R}}(\boldsymbol{r}) = E_{\mathrm{I}}(\boldsymbol{r}) = 0$, and the phase $\varphi(\boldsymbol{r}) = \arctan[E_{\mathrm{R}}(\boldsymbol{r})/E_{\mathrm{I}}(\boldsymbol{r})]$ is undefined.

2.2 Topological charge

According to the theory of crystal defects in materials science, we know that a single Burgers vector along a dislocation line is always conserved. Similar to the crystal structure, Nye and Berry have given the wave front dislocation (wave front defect) in the light wave field which is around the phase singularity along the dislocation line [1]

$$\frac{\lambda}{2\pi}\oint_C \nabla\varphi \cdot \mathrm{d}r = l\lambda, \tag{2}$$

where λ is wavelength, C is the closed curve around the phase singularity in the counterclockwise direction, φ is the phase, l denotes winding number which is also named topological charge [2], the magnitude of l is equal to the number of starting points of the helix plane around the phase singularity. Positive l represents the right hand spiral direction, negative l represents the left hand spiral direction. In Figs. 1(a) and 1(b), the starting points of the helix alleles around the phase singularity are 1 and 3, respectively, and the directions of the helix are all right-handed, so we can figure out that the l which contains the magnitude and the sign are + 1 and + 3, respectively. According to above definition, one finds that l in Figs. 1(c) and 1(d) is equal to −1 and −3, respectively.

2.3 Wave front dislocation

Wave front dislocation (or phase defect) mainly includes three types [1], namely, screw dislocation, edge dislocation and mixed edge-screw dislocation. The light wave field of the mixed edge-screw dislocation includes both screw dislocation and edge dislocation.

Screw dislocation, is also known as optical vortex (or vortex beam) in the optical field. It is known that a fully coherent beam can be characterized by the electric field. We may write this electric field of a fully coherent optical vortex beam with an arbitrary initial phase β (normally set to zero) at the source plane in polar representation in terms of an amplitude $A(\boldsymbol{r})$ and vortex phase structure $\exp(\mathrm{i}l\theta)$,

$$E_{\mathrm{V}}(\boldsymbol{r},\theta) = A(\boldsymbol{r})\exp(\mathrm{i}l\theta + \mathrm{i}\beta), \tag{3}$$

where l is the TC mentioned above, θ is the azimuthal angle. By modulating $A(\boldsymbol{r})$, one can obtain different fully coherent vortex beam, such as Gaussian vortex (GV) beam [128], Laguerre-Gaussian (LG) beam [5,129], anomalous vortex (AV) beam [9], high order Bessel-Gaussian (BG) beam [8] and perfect vortex (PV) beam [10]. Compared with plane wave, the main characteristics of optical vortex are helical wave front and phase singularity. At the points of these singularities of optical vortex where the intensity of the wave is zero and the phase is undefined. Take the GV beam as an example, we calculate in Fig. 2 the intensity and phase distributions of the GV beam with different l at the source plane. It shows that the optical vortex is a point defect, and the center is dark, that is, the intensity is zero, which is caused by the phase singularity. In addition, the sign of l is positive if the phase increases along anti-clockwise direction, whereas, negative if the phase increases along clockwise direction. If the phase changes (increases) $2\pi l$, the magnitude of TC is l [130], which can be an arbitrary value, both integral and fractional. All the phase lines intersect at the center of the optical vortex, namely, the center of the optical vortex and any other point are all on the same contour of constant phase. Therefore, the phase at the center of the vortex is undefined. Note that vortex beam with fractional topological charge possesses a radial opening in the annular intensity ring during propagation, which is different from that at the source plane.

Edge dislocation, namely, pure dislocation line, whose prominent feature is that there is a straight dislocation line (incision) in the transverse plane along the propagation

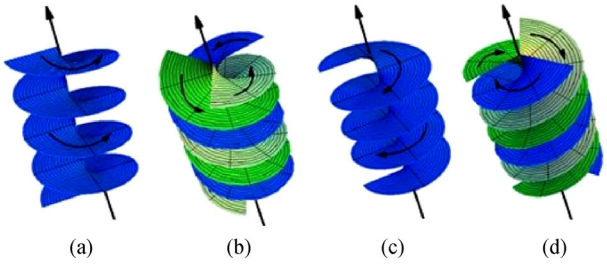

Fig. 1 Wave front of spiral structure. (a) and (b) Wave front of right hand spiral structure with topological charge l = 1 and 3; (c) and (d) wave front of left hand spiral structure with topological charge l = −1 and −3

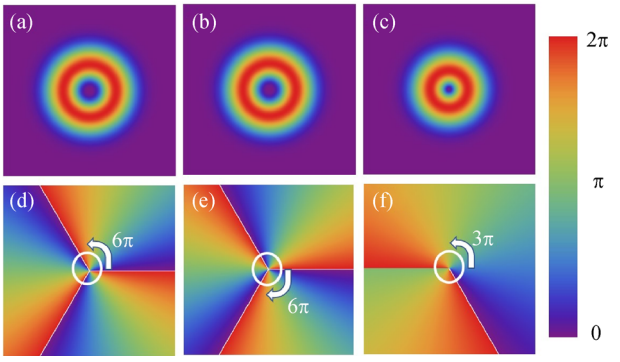

Fig. 2 Intensity and phase of Gaussian vortex beam with different l at the source plane. (a) and (d) $l = 3$; (b) and (e) $l = -3$; (c) and (f) $l = 1.5$

direction, and it has a jump by π in the phase between the two sides of the incision. In Cartesian coordinates, the electric field of a beam with edge dislocation at the source plane can be expressed as

$$E_{\mathrm{E}}(\boldsymbol{r}) = (px - y + d)f(\boldsymbol{r}), \tag{4}$$

where p and d are the slope and the off-axis distance of edge dislocation, $f(\boldsymbol{r})$ denotes the background light field distribution. We show the phase distribution of edge dislocation in Fig. 3.

2.4 Correlation singularities

It is well known that light fields which are partially coherent typically do not possess regions of zero intensity and hence do not possess any obvious phase singularities [87]. It is of interest to ask whether or not such fields possess singularities in some 'hidden' form. In 2003, Bogatyryova et al. [131] exhibited the vortex nature of partially coherent singular beam with a separable phase and studied the phase singularities of the spectral degree of coherence. Figure 4 shows the modulus and contours of constant phase of the spectral degree of coherence (correlation function) of a partially coherent beam with vortex phase superposed by LG_{01} and LG_{11} model beams. We can find from Fig. 4 when the modulus of the correlation function is 0, the phase will undergo a jump at that place, and is undefined as the correlation singularity. Later, Gbur et al. [86,89] further confirmed the existence of this hidden singularity (or hidden vortex), a good candidate for such hidden vortices is the singularities of two-point correlation functions described, so-called coherence vortices or correlation singularities [89]. Such vortices are pairs of points ($\boldsymbol{r}_1$ and $\boldsymbol{r}_2$) at which the spectral degree of coherence of the field vanishes, i.e., where

$$u(\boldsymbol{r}_1,\boldsymbol{r}_2) \equiv \frac{W(\boldsymbol{r}_1,\boldsymbol{r}_2)}{\sqrt{S(\boldsymbol{r}_1)S(\boldsymbol{r}_2)}} = 0, \tag{5}$$

or, equivalently, where

$$\mathrm{Re}[W(\boldsymbol{r}_1,\boldsymbol{r}_2)] = 0, \tag{6}$$

$$\mathrm{Im}[W(\boldsymbol{r}_1,\boldsymbol{r}_2)] = 0. \tag{7}$$

Here $W(\boldsymbol{r}_1,\boldsymbol{r}_2)$ denotes the mutual coherence function (cross-spectral density [132]) which is used to characterize the statistic properties of the partially coherent beam, but at which the spectral density (often referred to as intensity) $S(\boldsymbol{r}_i) = W(\boldsymbol{r}_i,\boldsymbol{r}_i)$ $(i = 1,2)$ of the field is nonzero. Re and Im denote taking the real and imaginary parts, respectively.

In 2004, Palacios et al. verified the existence of a robust correlation singularity in experiment [133]. Figure 5 shows the intensity and cross correlation functions of a partially coherent vortex beam with $l = 1$ in the far-field plane with different coherence lengths. One sees that the dark vortex core disappears as the coherence length decreases. However, a ring dislocation appears in the cross-correlation function, and with the decrease of coherence length, the radial size of ring dislocation increases and becomes more recognizable. It is similar to Fig. 3, the place where the correlation function is 0 (i.e., dark ring dislocation), the phase will undergo a π phase jump across the boundary.

Fig. 3 Phase of edge dislocation

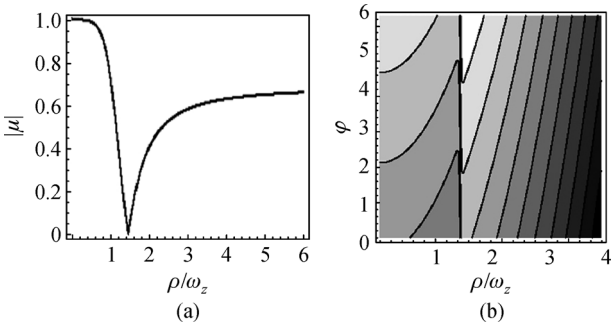

Fig. 4 (a) Modulus and (b) contours of constant phase of the spectral degree of coherence (correlation function) of a partially coherent beam with vortex phase superposed by LG_{01} and LG_{11} model beams [131]

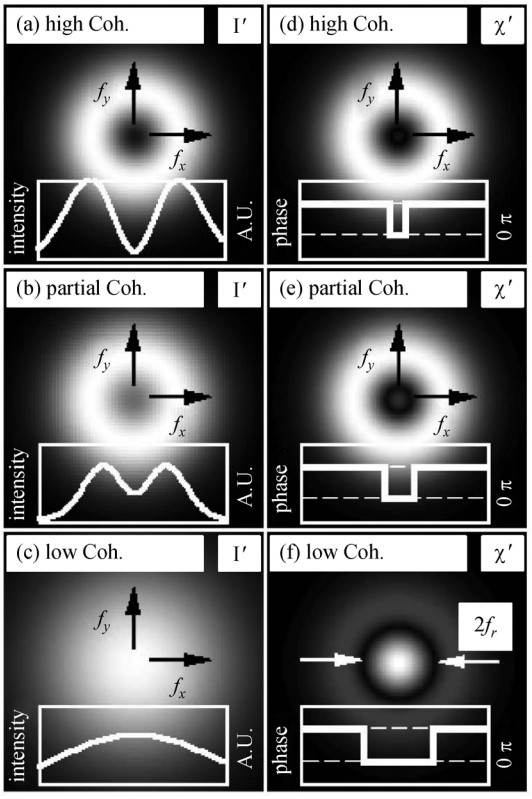

Fig. 5 Intensity (a–c) and cross correlation functions (d–f) of a partially coherent vortex beam with $l = 1$ in the far-field plane with different coherence lengths [133]

Therefore, a partially coherent vortex beams possess singularities with these two hidden forms, i.e., coherence vortices (or correlation vortices) and ring dislocations.

3 Theoretical models of partially coherent vortex beams

Considering the polarization characteristics, we divide partially coherent vortex beams into scalar partially coherent vortex beam and vector partially coherent vortex beam (including vector partially coherent vortex beams with uniform state of polarization and nonuniform state of polarization). Considering the correlation function, we divide partially coherent vortex beams into partially coherent vortex beam with conventional correlation function (i.e., Gaussian-correlated Schell model correlation) and partially coherent vortex beam with nonconventional correlation function (i.e., non-Gaussian-correlated Schell model correlation). Considering the value of topological charge, we divide partially coherent vortex beams into partially coherent integral vortex (PCIV) beam and partially coherent fractional vortex (PCFV) beam.

3.1 Theoretical models of a scalar partially coherent vortex beam with conventional correlation function

Unlike the case of fully coherent optical vortex beam (optical vortex) described in the previous section (Eq. (3)), the initial phase β of partially coherent vortex beam are random, it is generally accepted that a partially coherent beam can be characterized by its statistic properties (i.e., mutual coherence function (MCF) in the space-time domain or the CSD in the space-frequency domain) [132]. The CSD of a partially coherent vortex beam at the source plane is defined as a two-point correlation function, i.e.,

$$W(\boldsymbol{r}_1,\boldsymbol{r}_2) = \langle E_{\mathrm{V}}(\boldsymbol{r}_1)E_{\mathrm{V}}^{*}(\boldsymbol{r}_2)\rangle, \tag{8}$$

where $\boldsymbol{r}_1$ and $\boldsymbol{r}_2$ are the position vectors at the source plane, the angular brackets denote an ensemble average and the asterisk denotes the complex conjugate.

On substituting from Eq. (3) into Eq. (8), we can obtain the theoretical model of a partially coherent vortex beam

$$W(\boldsymbol{r}_1,\boldsymbol{r}_2) = A(\boldsymbol{r}_1)A(\boldsymbol{r}_2)g(\boldsymbol{r}_1-\boldsymbol{r}_2)\exp[\mathrm{i}l(\theta_1-\theta_2)], \tag{9}$$

where $g(\boldsymbol{r}_1-\boldsymbol{r}_2)$ denotes the correlation function [132] between two points $\boldsymbol{r}_1$ and $\boldsymbol{r}_2$. It is generally accepted that for the Carter-Wolf source [134], the correlation function satisfying the Gaussian-correlated Schell-model function and can be expressed as follows

$$g(\boldsymbol{r}_1-\boldsymbol{r}_2) = \exp\left[-\frac{(\boldsymbol{r}_1-\boldsymbol{r}_2)^2}{2\sigma_g^2}\right], \tag{10}$$

where σ_g denotes the initial coherence length. If we set $\sigma_g \to 0$, the beam source reduces to an incoherent beam, If we set $\sigma_g \to \infty$, the beam source becomes to a fully coherent beam. By modulating $A(\boldsymbol{r})$, one can obtain different partially coherent vortex beams with Gaussian correlated Schell-model function, such as Gaussian Schell-model vortex beam, Laguerre Gaussian Schell-model, Bessel Gaussian Schell-model beam.

If we set [128]

$$A(\boldsymbol{r}) = \exp\left(-\frac{\boldsymbol{r}^2}{w_0^2}\right), \tag{11}$$

where w_0 is the beam waist. By substituting Eqs. (10) and (11) into Eq. (9), the CSD function of the basic Gaussian Schell-model vortex (GSMV) beam takes the form

$$W_{\mathrm{GSMV}}(\boldsymbol{r}_1,\boldsymbol{r}_2) = \exp\left[-\frac{\boldsymbol{r}_1^2+\boldsymbol{r}_2^2}{w_0^2}-\frac{(\boldsymbol{r}_1-\boldsymbol{r}_2)^2}{2\delta_g^2}\right]\exp[\mathrm{i}l(\theta_1-\theta_2)]. \tag{12}$$

If we set [5,129]

$$A(\boldsymbol{r}) = \left(\frac{\sqrt{2}\boldsymbol{r}}{w_0}\right)^l L_p^l\left(-\frac{2\boldsymbol{r}^2}{w_0^2}\right)\exp\left(-\frac{\boldsymbol{r}^2}{w_0^2}\right), \quad (13)$$

where L_p^l denotes the Laguerre polynomial with mode orders p and l. By substituting Eqs. (10) and (13) into Eq. (7), the CSD function of the Laguerre Gaussian Schell-model (LGSM) beam can be expressed as

$$W_{\mathrm{LGSM}}(\boldsymbol{r}_1,\boldsymbol{r}_2) = \left(\frac{2\boldsymbol{r}_1\boldsymbol{r}_2}{w_0^2}\right)^l L_p^l\left(-\frac{2\boldsymbol{r}_1^2}{w_0^2}\right)L_p^l\left(-\frac{2\boldsymbol{r}_2^2}{w_0^2}\right) \exp\left[-\frac{\boldsymbol{r}_1^2+\boldsymbol{r}_2^2}{w_0^2}-\frac{(\boldsymbol{r}_1-\boldsymbol{r}_2)^2}{2\sigma_g^2}\right]\exp[\mathrm{i}l(\theta_1-\theta_2)]. \quad (14)$$

If we set [9]

$$A(\boldsymbol{r}) = \left(\frac{\boldsymbol{r}}{w_0}\right)^{2n+|l|}\exp\left(-\frac{\boldsymbol{r}^2}{w_0^2}\right), \quad (15)$$

where n is the beam order of the anomalous vortex beam. By substituting Eqs. (10) and (15) into Eq. (9), the CSD function of the anomalous Gaussian Schell-model vortex (AGSMV) beam can be expressed as

$$W_{\mathrm{AGSMV}}(\boldsymbol{r}_1,\boldsymbol{r}_2) = \left(\frac{\boldsymbol{r}_1\boldsymbol{r}_2}{w_0^2}\right)^{2n+|l|}\exp\left[-\frac{\boldsymbol{r}_1^2+\boldsymbol{r}_2^2}{w_0^2}-\frac{(\boldsymbol{r}_1-\boldsymbol{r}_2)^2}{2\sigma_g^2}\right]\exp[\mathrm{i}l(\theta_1-\theta_2)]. \quad (16)$$

If we set [8]

$$A(\boldsymbol{r}) = J_l(\beta_0\boldsymbol{r})\exp\left(-\frac{\boldsymbol{r}^2}{w_0^2}\right), \quad (17)$$

where β_0 is the radial frequency, J_l is the Bessel function of first kind with order l. When $l \geqslant 1$, J_l represents the high order Bessel function. By substituting Eqs. (10) and (17) into Eq. (9), one can obtain the CSD function of the Bessel Gaussian Schell-model (BGSM) beam as follows

$$W_{\mathrm{BGSM}}(\boldsymbol{r}_1,\boldsymbol{r}_2) = J_l(\beta_0\boldsymbol{r}_1)J_l(\beta_0\boldsymbol{r}_2) \exp\left[-\frac{\boldsymbol{r}_1^2+\boldsymbol{r}_2^2}{w_0^2}-\frac{(\boldsymbol{r}_1-\boldsymbol{r}_2)^2}{2\sigma_g^2}\right]\exp[\mathrm{i}l(\theta_1-\theta_2)]. \quad (18)$$

3.2 Theoretical models of a scalar partially coherent vortex beam with nonconventional correlation function

According to the Gori's pioneering work [106], it is found that the correlation function of a partially coherent beam is not limited to the Gaussian correlated Schell-model function. In fact, partially coherent beams with conventional correlation function can be proposed and generated [135]. Chen et al. have introduced and generated one kind of partially coherent vortex beam with nonconventional correlation function named Laguerre-Gaussian correlated Schell-model vortex (LGCSMV) beam [113], whose CSD function is expressed as

$$W_{\mathrm{LGCSMV}}(\boldsymbol{r}_1,\boldsymbol{r}_2) = \exp\left[-\frac{\boldsymbol{r}_1^2+\boldsymbol{r}_2^2}{w_0^2}-\frac{(\boldsymbol{r}_1-\boldsymbol{r}_2)^2}{2\sigma_g^2}\right] L_p^0\left[\frac{(\boldsymbol{r}_1-\boldsymbol{r}_2)^2}{2\sigma_g^2}\right]\exp[\mathrm{i}l(\theta_1-\theta_2)], \quad (19)$$

where L_p^0 represents the Laguerre polynomial with mode orders p and $l = 0$. We will use the experimental setup in Fig. 8 below to generate a LGCSMV beam represented by Eq. (19). If we set $p = 0$, Eq. (19) reduces to the GSMV beam. Due to the vortex phase, the LGCSMV beam exhibits unique propagation properties which are much different from those of the GSMV beam.

3.3 Theoretical models of a vector partially coherent vortex beam

The research scope of partially coherent vortex beam has been extended from scalar light field to vector light field. Unlike a scalar partially coherent beam, it is well known that a vector partially coherent beam can be characterized by the CSD matrix.

Electromagnetic Gaussian Schell-model vortex (EGSMV) beam is a typical kind of vector partially coherent vortex beam with uniform state of polarization, whose CSD matrix in the source plane is given as [115]

$$\overleftrightarrow{W}_{\mathrm{EGSMV}}(\boldsymbol{r}_1,\boldsymbol{r}_2) = \begin{pmatrix} W_{xx}(\boldsymbol{r}_1,\boldsymbol{r}_2) & W_{xy}(\boldsymbol{r}_1,\boldsymbol{r}_2) \\ W_{yx}(\boldsymbol{r}_1,\boldsymbol{r}_2) & W_{yy}(\boldsymbol{r}_1,\boldsymbol{r}_2) \end{pmatrix}, \quad (20)$$

where $W_{\alpha\beta}(\boldsymbol{r}_1,\boldsymbol{r}_2) = \langle E_\alpha^*(\boldsymbol{r}_1)E_\beta(\boldsymbol{r}_2)\rangle$, $(\alpha,\beta = x,y)$. The elements of the CSD matrix are expressed as follows:

$$W_{\alpha\beta}(\boldsymbol{r}_1,\boldsymbol{r}_2) = A_\alpha A_\beta B_{\alpha\beta}\exp\left[-\frac{\boldsymbol{r}_1^2}{4\delta_\alpha^2}-\frac{\boldsymbol{r}_2^2}{4\delta_\beta^2}-\frac{(\boldsymbol{r}_1-\boldsymbol{r}_2)^2}{2\sigma_{\alpha\beta}^2}\right]\exp[\mathrm{i}l(\theta_1-\theta_2)], \quad (21)$$

where A_x and A_y are the amplitudes of x and y components of the electric field, respectively. $B_{xx} = B_{yy} = 1$, $B_{xy} = |B_{xy}|\exp(\mathrm{i}\phi_{xy})$ is the complex correlation coefficient between the x and y components of the electric field with ϕ_{xy} being the phase difference between the x and y components. δ_i denotes the r.m.s width of the intensity distribution along the i direction, σ_{xx}, σ_{yy} and σ_{xy} are the

r.m.s widths of autocorrelation function of the x component of the electric field, of the y component of the electric field and of the mutual correlation function of x and y components of the electric field, respectively.

Partially coherent radially polarized vortex beam is a typical vector partially coherent vortex beam with nonuniform state of polarization. The elements of the partially coherent radially polarized vortex beam are expressed as [117]

$$W_{xx}(\boldsymbol{r}_1,\boldsymbol{r}_2) = \frac{r_1 r_2 \cos\theta_1 \cos\theta_2}{w_0^2} T, \tag{22}$$

$$W_{xy}(\boldsymbol{r}_1,\boldsymbol{r}_2) = \frac{r_1 r_2 \cos\theta_1 \sin\theta_2}{w_0^2} T, \tag{23}$$

$$W_{yx}(\boldsymbol{r}_1,\boldsymbol{r}_2) = W_{xy}^*(\boldsymbol{r}_1,\boldsymbol{r}_2), \tag{24}$$

$$W_{yy}(\boldsymbol{r}_1,\boldsymbol{r}_2) = \frac{r_1 r_2 \sin\theta_1 \sin\theta_2}{w_0^2} T, \tag{25}$$

where

$$T = \exp\left(-\frac{\boldsymbol{r}_1^2 + \boldsymbol{r}_2^2}{w_0^2}\right) \exp\left[-\frac{(\boldsymbol{r}_1 - \boldsymbol{r}_2)^2}{2\sigma_g^2}\right] \exp[\mathrm{i}l(\theta_1 - \theta_2)]. \tag{26}$$

3.4 Theoretical models of a partially coherent fractional vortex beam

Above theoretical models are limited to partially coherent vortex beam with integral TC, and in fact, the value of TC can be non-integral (i.e., fractional TC), namely, l can be an arbitrary value, both integral and fractional. By choosing a fractional value of l, above equations represents the CSD functions of corresponding partially coherent fractional vortex beams. We have introduced partially coherent fractional vortex beam as a natural extension of coherent fractional vortex beam in Ref. [120], while it is hard to derive analytical propagation formula for a partially coherent fractional vortex beam due to fractional value of l, we have to resort to numerical integration.

4 Generation of partially coherent vortex beams

The conventional way of generating a partially coherent vortex beam is to produce a partially coherent source first, and then we add the vortex phase with the help of spiral phase plate (SPP) [28], spatial light modulator (SLM) [30] or digital micromirror device (DMD) [136] to a partially coherent source to generate a partially coherent vortex beam. It was shown in [137] that a partially coherent source can be produced starting with a spatial incoherent source and using a collimating lens and an amplitude filter. For creating the spatial incoherent source, people use, for example, the rotating ground-glass disk (RGGD) [94], the SLM [138], and the DMD [136] to produce the incoherent beam. This paper mainly introduces the method for generating a partially coherent vortex beam by using a RGGD.

4.1 Generation of a scalar partially coherent vortex beam with conventional correlation function

Figure 6 shows the experimental setup for generating a Gaussian Schell-model vortex (GSMV) beam [94]. A light beam from a He-Ne laser first propagates through the neutral density filter (NDF). The transmitted beam is focused by a thin lens L_1 and then illuminates a rotating ground-glass disk (RGGD), producing a partially coherent beam with Gaussian statistics. The thin lens L_2 is used to collimate the transmitted light, and the Gaussian amplitude filter (GAF) is used to transform the intensity of the transmitted light into a Gaussian profile. The transmitted beam behind the GAF is a GSM beam. The transverse beam width of the GSM beam is determined by the transmission function of the GAF. The transverse coherence width of the GSM beam is determined by the roughness of the RGGD and the focused beam spot size on the RGGD together. In our experiment, the roughness of the RGGD is fixed. We mainly modulate the transverse coherence width of the GSM beam by varying the focused beam spot size on the RGGD. After passing through a spiral phase plate (SPP) with topological charge $l = 1$ located just behind the GAF, the GSM beam becomes a GSMV beam with $l = 1$.

Figure 7(a) shows the experimental setup for generating a Laguerre Gaussian Schell-model (LGSM) beam [139]. In this way, the generation process is similar to that shown in Fig. 6, the only difference is that we used a spatial light modulator (SLM) to load the corresponding fork interference pattern with different topological charge l and radial mode p (i.e., hologram of interference between plane wave and LG beam). Similarly, if we replace above fork interference pattern with the corresponding holograms, we can also obtain the anomalous Gaussian Schell-model

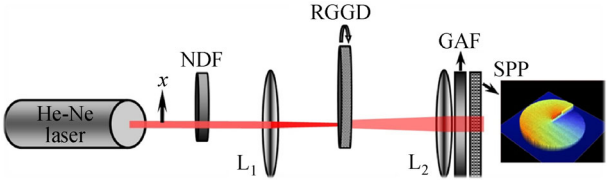

Fig. 6 Experimental setup for generating a Gaussian Schell-model vortex beam [94]. NDF, neutral density filter; RGGD, rotating ground-glass disk; GAF, Gaussian amplitude filter; SPP, spiral phase plate; L_1, L_2, lenses

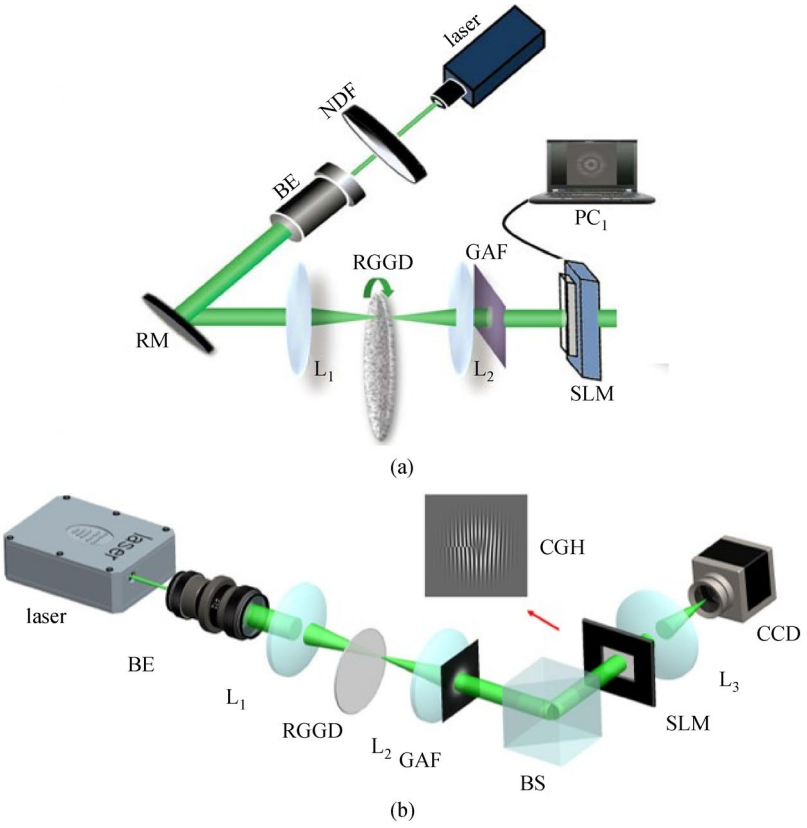

Fig. 7 (a) Experimental setup for generating a LG_{pl} beam [139]; (b) experimental setup for generating a partially coherent fractional vortex beam [120]. NDF, neutral density filter; BE, beam expander; RM, reflecting mirror; L_1, L_2, L_3, thin lenses; PC_1, personal computers; RGGD, rotating ground-glass disk; GAF, Gaussian amplitude filter; SLM, spatial light modulator; CA, circular aperture; BS, beam splitter; CGH, computer-generated holograms; CCD: charge-coupled device

vortex (AGSMV) beam and Bessel Gaussian Schell-model (BGSM) beam.

Figure 7(b) shows our experimental setup for generating partially coherent fractional vortex beam [120]. The generation is the same as shown in Fig. 7(a), the biggest difference is that we used a fractional order fork interference pattern to replace an integral order fork interference pattern.

4.2 Generation of a scalar partially coherent vortex beam with nonconventional correlation function

In this section, we generate a LGCSMV beam [113] through conversion of a LGCSM beam with the help of a SPP, which means that we have to generate a LGCSM beam first, then to add a vortex phase on a LGCSM beam. The generation is the same as shown above, the biggest difference is that we need to transform the intensity distribution of the light source into a dark hollow beam before it reaches the lens L_1, the rationality of this experimental scheme has been confirmed by literature [140]. The pattern of the phase grating loaded on the SLM is obtained by computing the interference pattern between a plane wave (reference wave) and a dark hollow beam. The phase grating for generating a dark hollow beam with $l = 1$ is shown as inset in Fig. 8. The circular aperture (CA) put here is used to select out the first order of the beam from the SLM (i.e., a dark hollow beam with $l = 1$). After passing through a thin lens L_1, the generated dark hollow beam by a SLM illuminates a RGGD, producing an incoherent beam with dark hollow beam profile [140]. The GAF is used to transform generated incoherent dark hollow beam into a LGCSM beam. The SPP is used to load vortex phase to the generated LGCSM beam to produce LGCSMV beam. Similarly, if we change the above interference pattern, we can also obtain the partially coherent vortex beams with different nonconventional correlation functions [135,140].

4.3 Generation of a vector partially coherent vortex beam

Vector partially coherent vortex beams can be divided into two types, i.e., a vector partially coherent vortex beam with uniform state of polarization and a vector partially coherent vortex beam with nonuniform state of polarization.

Electromagnetic Gaussian Schell model vortex beam is a typical vector partially coherent vortex beam with uniform state of polarization. If the antidiagonal elements of the

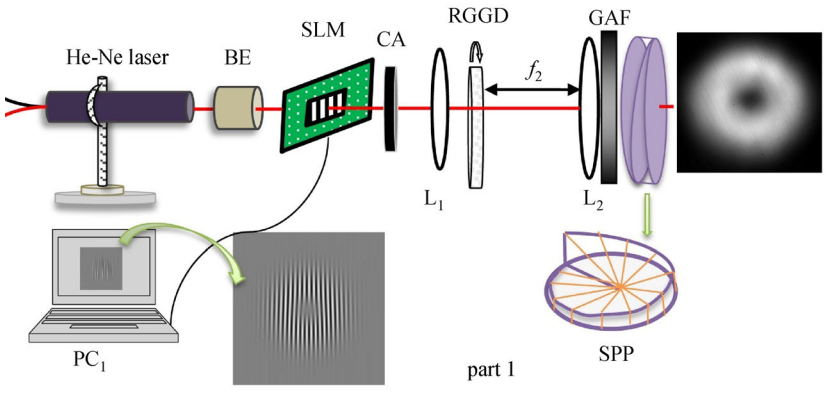

Fig. 8 Experimental setup for generating a Laguerre-Gaussian correlated Schell-model vortex beam [113]. BE, beam expander; SLM, spatial light modulator; CA, circular aperture; RGGD, rotating ground-glass disk; GAF, Gaussian amplitude filter; L_1, L_2, thin lenses; SPP, spiral phase plate; PC_1, personal computers

CSD matrix are zero (i.e., $B_{xy} = 0$), which means the x and y components of the beam source are uncorrelated, then we can use superposition of two independent of linear polarization beams to generate this kind of beam source as shown in Fig. 9(a). Here we use two different laser source and RGGD to make sure that the x and y components is uncorrelated. If the antidiagonal elements are nonzero (i.e., $B_{xy} \neq 0$), we can use a Mach-Zehnder inter-ferrometer to generate this kind of beam source as shown in Fig. 9(b). The detailed information can be found in Ref. [115].

Partially coherent radially polarized vortex beam is a typical kind of vector partially coherent vortex beam with nonuniform state of polarization. Figure 10 shows the experiment setup for generating partially coherent radially polarized vortex beam, which is similar to the setup for generating GSMV beam. The only difference is that the addition of a radially polarized convertor (RPC) between GAF and SPP, which is used to convert the generated linearly polarized GSM beam to a radially polarized GSM beam. The detailed information can be found in Ref. [117].

5 Propagation properties and application of partially coherent vortex beams

Partially coherent vortex beams exhibit unique optical properties on propagation, such as beam shaping, beam rotation and self-reconstruction, which are much different from fully coherent vortex beam and partially coherent beam without vortex phase.

5.1 Beam shaping

Figures 11 – 13 show the intensity distribution and the corresponding cross line (y = 0) of focused partially

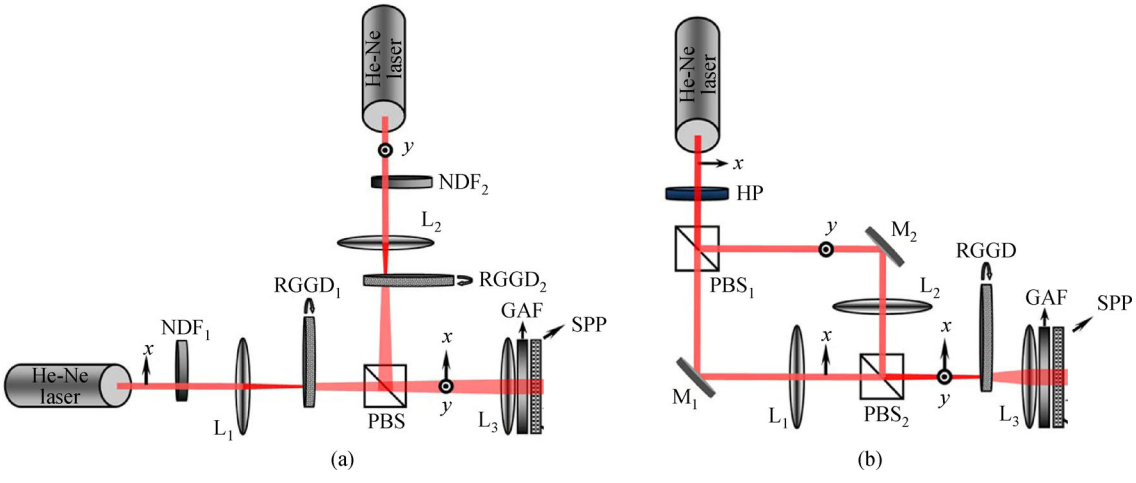

Fig. 9 Experimental setup for generating a vector partially coherent vortex beam with uniform state of polarization [115]. (a) Without antidiagonal elements; (b) with antidiagonal elements. NDF_1, NDF_2, neutral density filters; L_1, L_2, thin lenses; $RGGD_1$, $RGGD_2$, rotating ground-glass disks; PBS, polarization beam splitter; GAF, Gaussian amplitude filter; SPP, spiral phase plate; HP, half-wave plate; M_1, M_2, reflecting mirrors

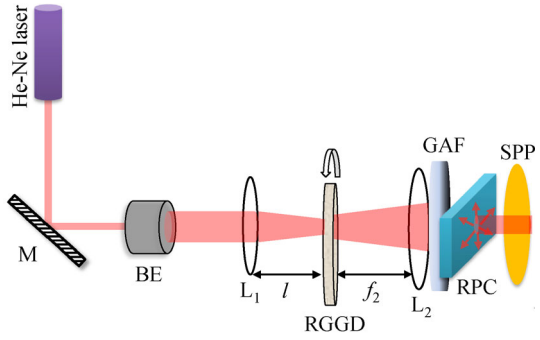

Fig. 10 Experimental setup for generating a partially coherent radially polarized vortex beam [117]. M, reflecting mirror; BE, beam expander; L_1, L_2, thin lenses; RGGD, rotating ground-glass disk; GAF, Gaussian amplitude filter; RPC, radially polarized convertor; SPP, spiral phase plate

coherent vortex beam in the focal plane with different values of the initial coherence length, the topological charge and the initial degree of polarization. It is found that we can shape the beam profile (i.e., dark hollow, flat-topped, and Gaussian beam spot) of the focused partially coherent vortex beam by varying its initial coherence length, topological charge and initial degree of polarization, which is useful for optical trapping [118].

5.2 Beam rotation

Figure 14 shows the normalized intensity distributions of a partially coherent integral vortex (PCIV) beam and a partially coherent fractional vortex (PCFV) beam focused by a thin lens at several propagation distances z [120]. We infer from Fig. 14 that the intensity pattern of a PCFV beam is much different from that of a PCIV beam. The intensity pattern of a PCFV beam possesses a radial opening in the annular ring encompassing the dark core near the source plane ($z = 0.1f$), and the opening gap rotates clockwise as z increases (or rotates anticlockwise for negative l, which is not shown here), and up to 90° at the focal plane ($z = f$)

Figures 15 – 17 show the intensity distribution I and its components I_x and I_y of a focused partially coherent radially polarized vortex beam with different l ($l = 0$, 2 and −2) in the x-y plane at several propagation distances [117]. One sees that the beam spots of the I_x, I_y and I of a focused partially coherent radially polarized beam without vortex phase ($l = 0$) do not rotate on propagation (see Fig. 15). While the beam spots of the I_x, and I_y of a focused partially coherent radially polarized vortex beam rotate in anti-clockwise with $l = 2$ (see Fig. 16) and in clockwise with $l = -2$ (see Fig. 17) on propagation, which means the beam spot of I also rotates on propagation although it is not demonstrated in Figs. 16(a1)–16(e1) and Figs. 17(a1)–17(e1) because the beam spot is of circular symmetry. The rotation of the beam spot is induced by the vortex phase, which imposes angular orbital angular momentum on the beam. Therefore, we can rotate the beam by modulating the topological charge, which is used for optical tweezers. In addition, in Fig. 18, it is found that we can realize beam rotation by using special optical system (i.e., cylindrical optical system) [141], which is used for determining topological charge.

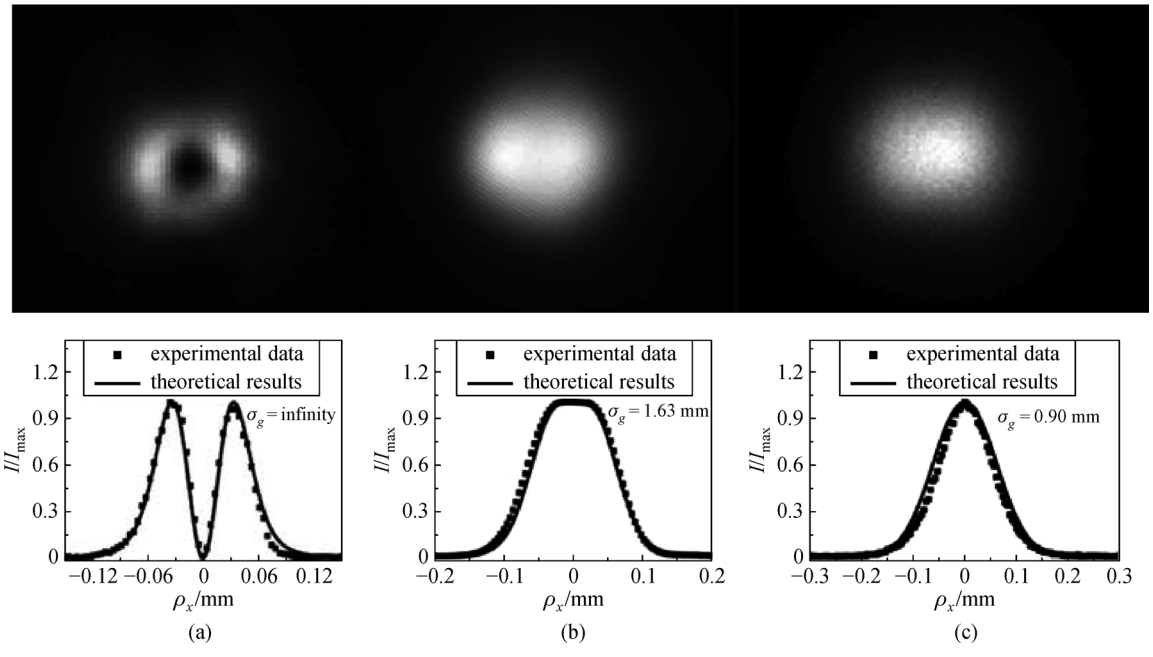

Fig. 11 Intensity distribution and the corresponding cross line ($y = 0$) of focused Gaussian Schell-model vortex beam in the focal plane for different values of initial coherence length σ_g [94]

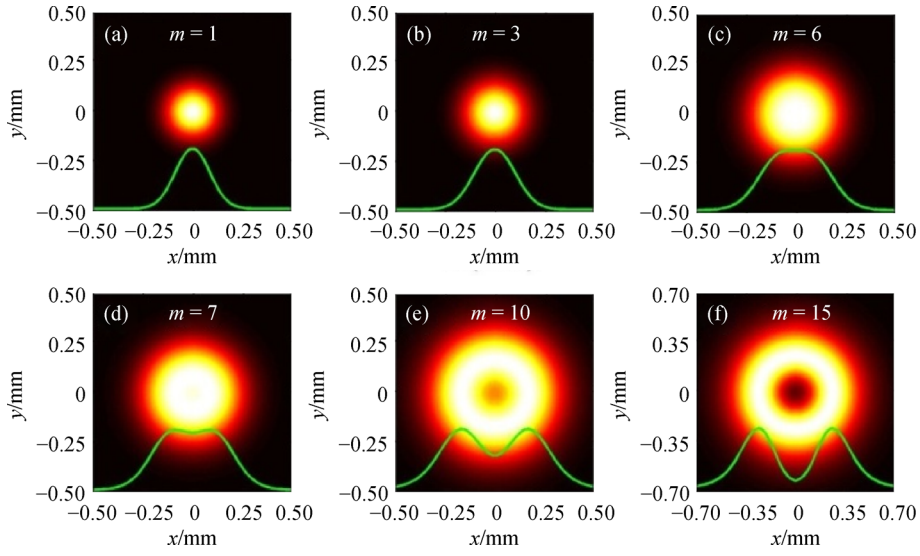

Fig. 12 Intensity distribution and the corresponding cross line ($y = 0$) of a focused partially coherent radially polarized vortex beam in the focal plane for different values of the topological charge m [117]

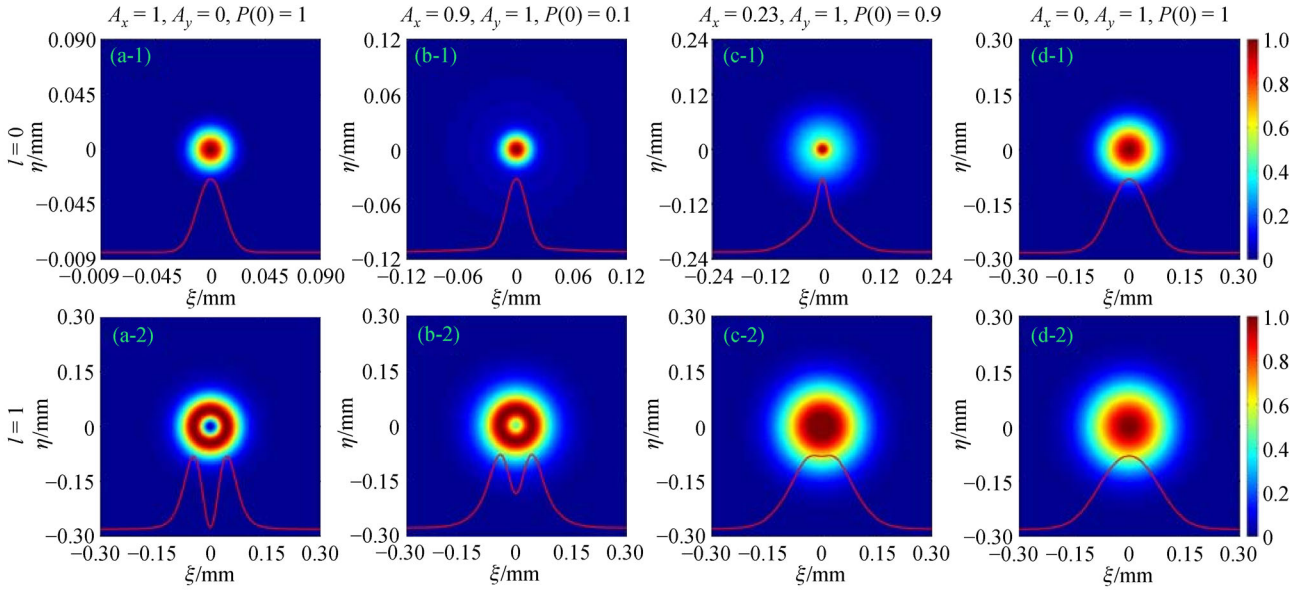

Fig. 13 Intensity distribution and the corresponding cross line ($y = 0$) of an electromagnetic Gaussian Schell-model beam without vortex phase and an electromagnetic Gaussian Schell-model vortex beam in the focal plane for different values of the initial degree of polarization [115]

5.3 Self-reconstruction

In addition to above mentioned intensity properties (i.e., beam shaping and beam rotation) on propagation and the correlation singularity above, a partially coherent vortex beam has another propagation property, i.e., self-reconstruction, which includes self-reconstruction of intensity and self-reconstruction of correlation function.

Figures 19 and 20 show the normalized intensity distribution and modulus of the degree of coherence of a focused partially Laguerre Gaussian (LG_{pl}) beam with $p = 1$ and $l = 1$ obstructed by a sector shaped opaque obstacle with center angle α at several propagation distances. Figure 21 shows the normalized intensity distribution and modulus of the degree of coherence obstructed by a sector shaped opaque obstacle with center angle $\alpha = 90°$ in the focal plane for different values of initial coherence length. One finds from Figs. 19(a1)–19(d1) that a focused partially coherent LG_{pl} beam exhibits a dark hollow beam profile in the source plane as $\alpha = 0°$, and with the

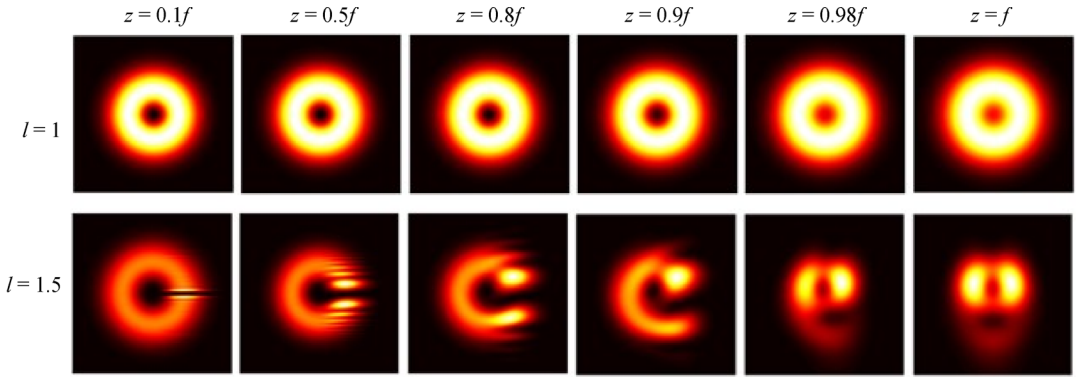

Fig. 14 Normalized intensity distributions of a PCIV beam (l = 1) and a PCFV beam (l = 1.5) focused by a thin lens at several propagation distances [120]

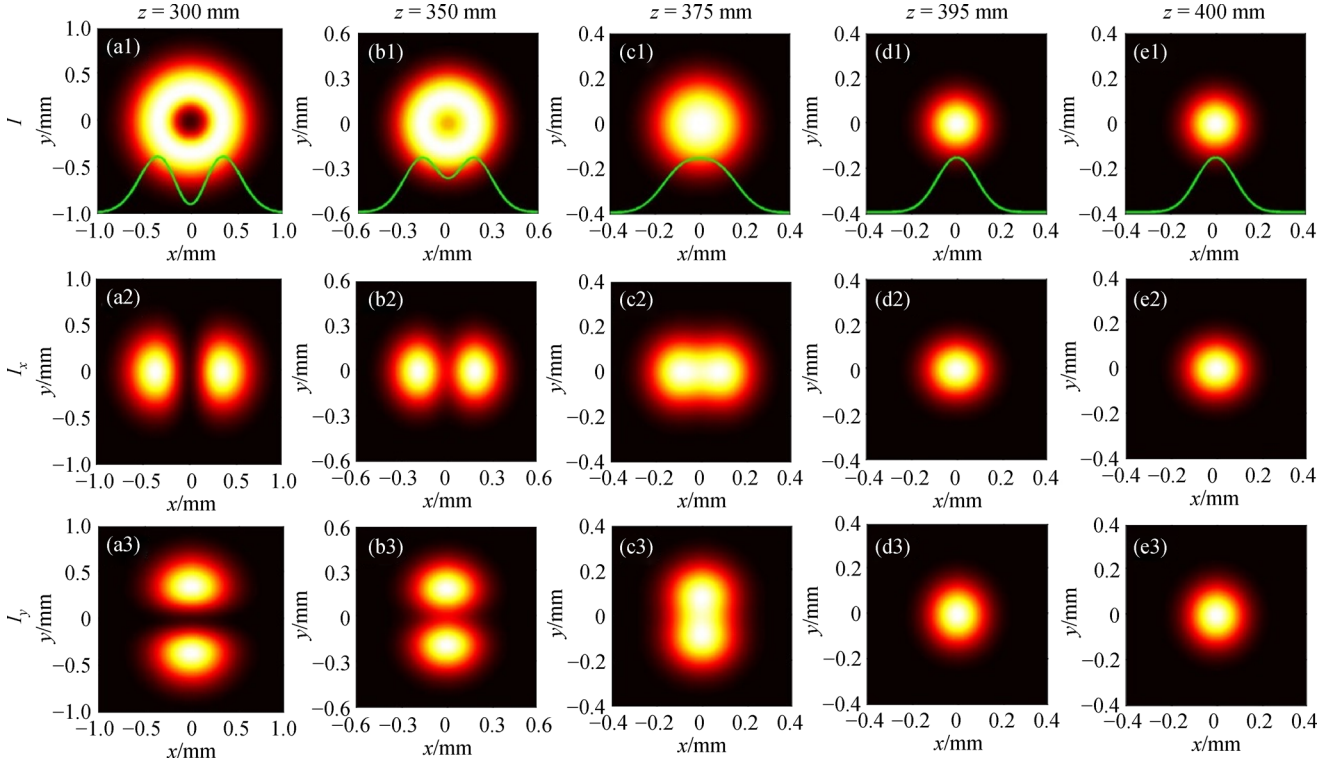

Fig. 15 Intensity distribution and its x- and y-components of a focused partially coherent radially polarized vortex beam with l = 0 in the x-y plane at several propagation distances. The green solid curve denotes the cross line (y = 0) [117]

increase of the propagation distance, the dark hollow beam profile gradually disappears, and finally becomes a Gaussian beam spot in the focal plane, while the intensity does not reveal any information. Fortunately, one sees that the distribution of the degree of coherence exhibits a Gaussian beam spot in the source plane, while it exhibits ring dislocation (i.e., correlation singularity) in the focal plane, and the number of ring dislocation is $N = 2p + |l|$, which reveals the information of topological charge. In Figs. 19(a2)–19(d3), it is seen that although the intensity distribution is partly blocked in the source plane, the intensity distribution gradually self-reconstructs on propagation, and finally becomes a Gaussian beam spot. The distribution of the degree of coherence also exhibits self-reconstruction ability on propagation, although with some distortion, but it is not hard to recognize that the number of dislocation also is $2p + |l|$. From Fig. 21, we can see that decreasing the initial coherence length will enhance the self-reconstruction ability and make the beam spot and ring dislocation more circular. Although self-reconstruction of intensity cannot reveal any information, but the self-reconstruction of correlation function can be used for

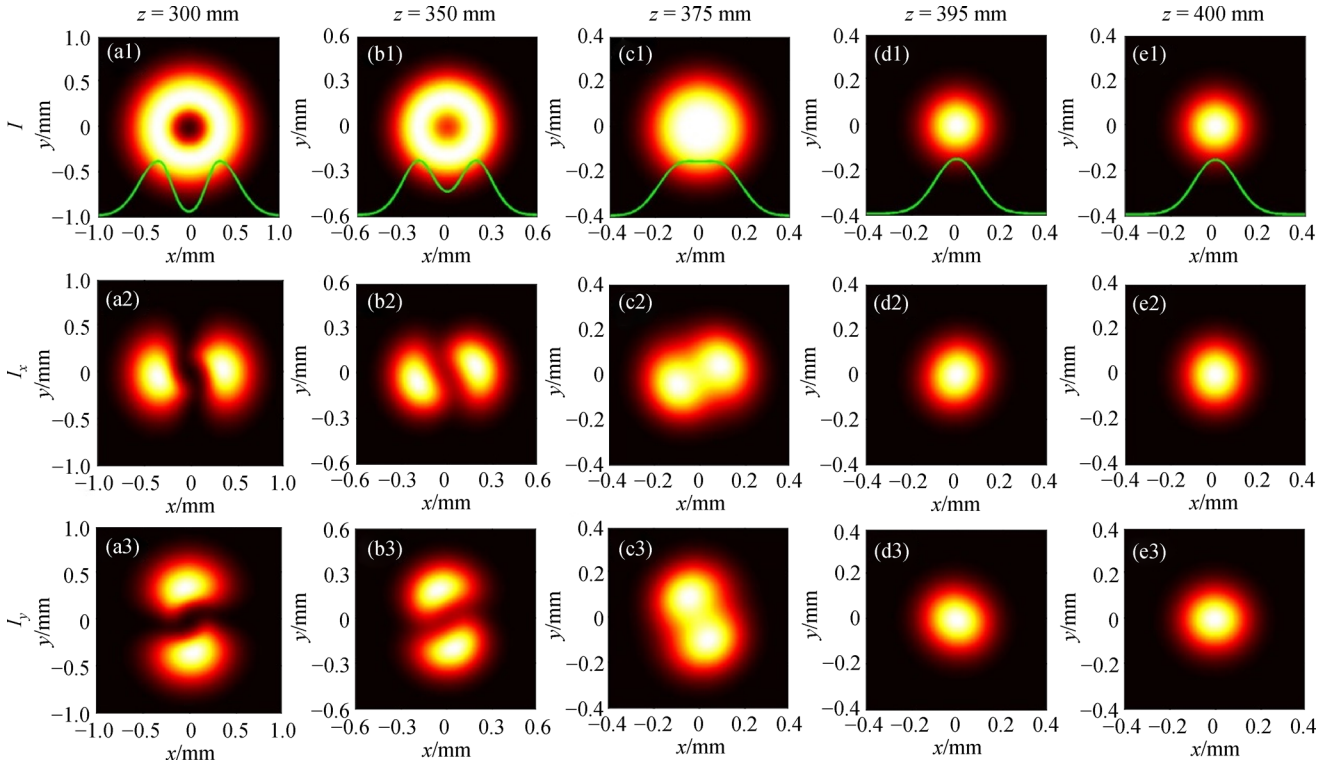

Fig. 16 Intensity distribution and its x- and y-components of a focused partially coherent radially polarized vortex beam with $l = 2$ in the x-y plane at several propagation distances. The green solid curve denotes the cross line ($y = 0$) [117]

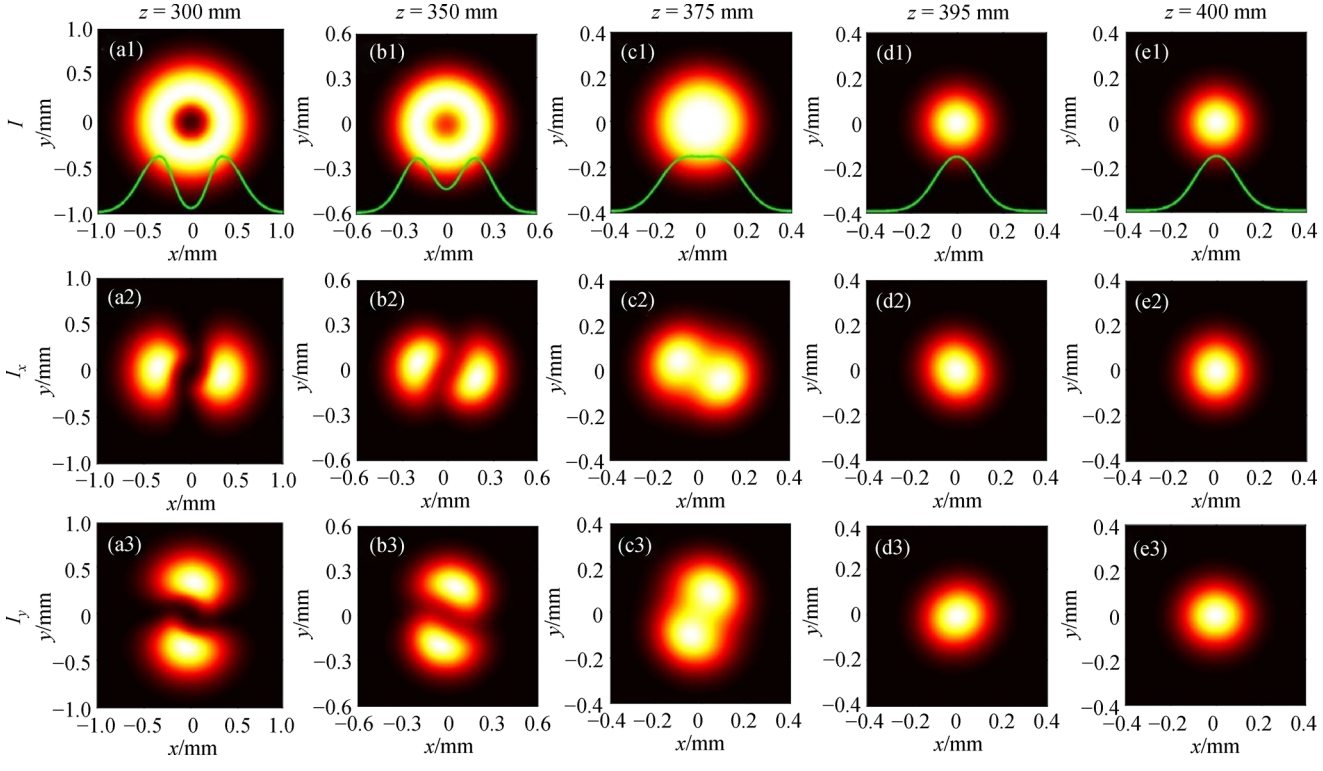

Fig. 17 Intensity distribution and its x- and y-components of a focused partially coherent radially polarized vortex beam with $l = -2$ in the x-y plane at several propagation distances. The green solid curve denotes the cross line ($y = 0$) [117]

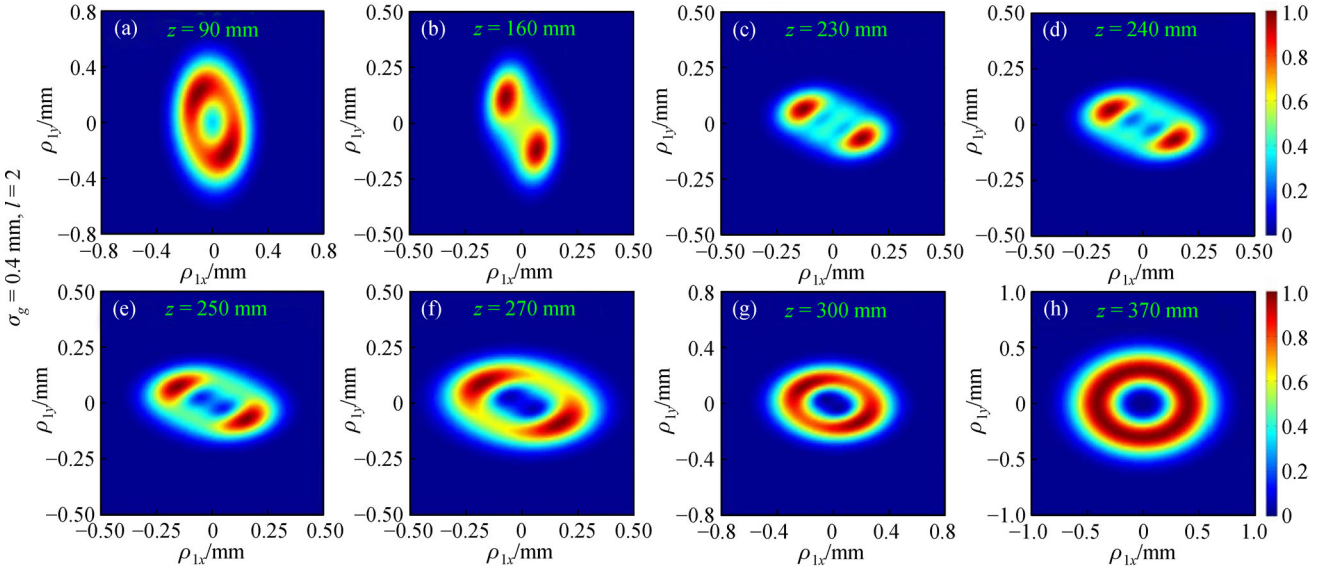

Fig. 18 Normalized average intensity distribution of a partially coherent LG_{0l} beam after passing through a couple of cylindrical lenses at different propagation distances [141]

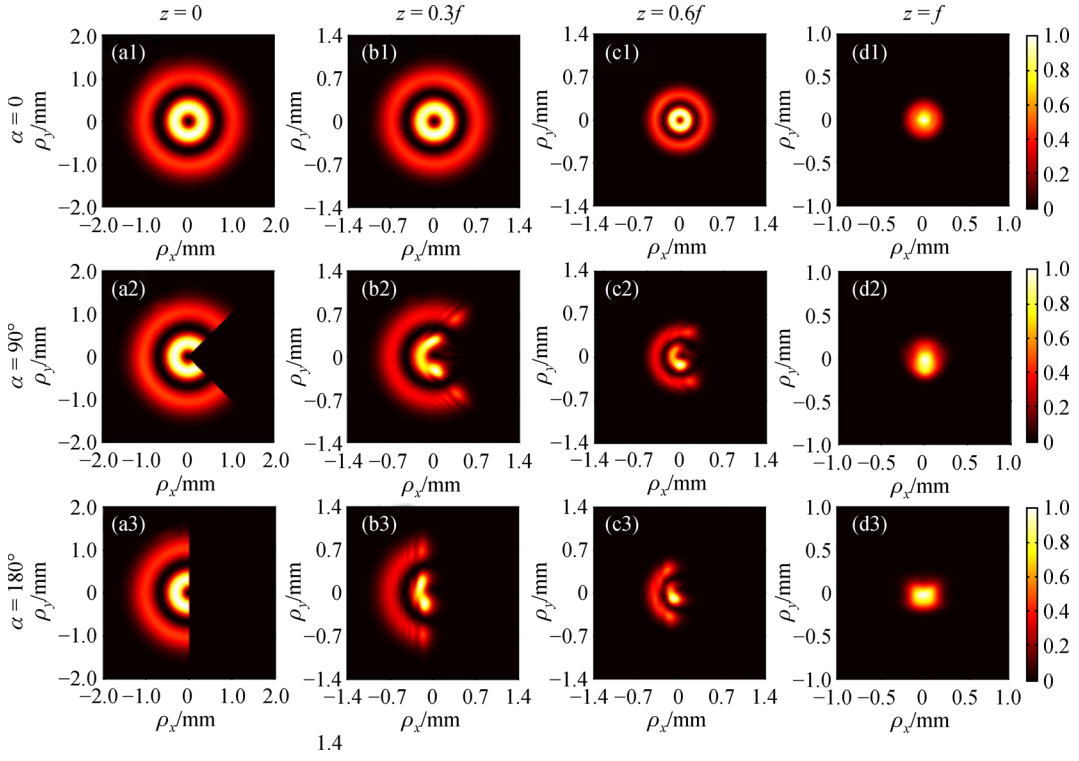

Fig. 19 Normalized intensity distribution of a focused partially coherent LG_{pl} beam with p = 1 and l = 1 obstructed by a sector shaped opaque obstacle with center angle α at several propagation distances [102]

measuring the topological charge of partially coherent vortex beam and information encryption and decryption.

Thus, in contrast with the non-diffracting beams (e.g., Airy or Bessel beams), the partially coherent beam has unique advantages in detecting information. Both of them have the property of self-reconstruction, however, the former only repair the intensity, and the intensity does not reveal all information of the beam source, such as topological charge. Fortunately, a partially coherent light cannot only repair the intensity, but also repair the correlation function which can reveal the information of topological charge.

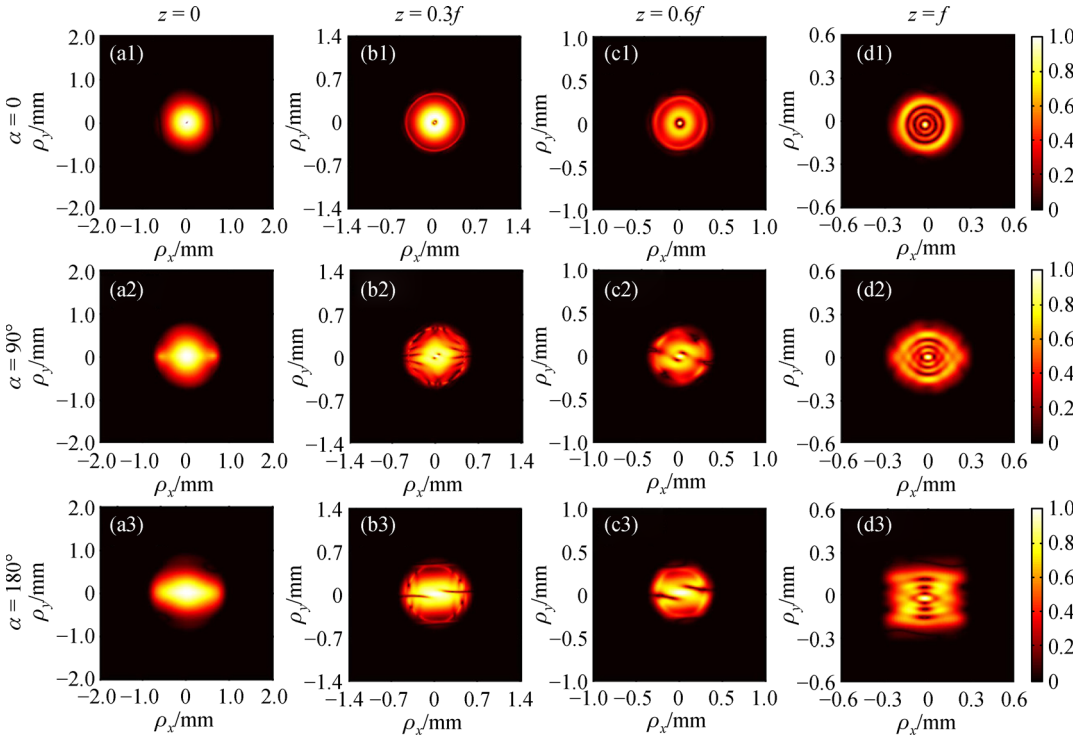

Fig. 20 Modulus of the degree of coherence of a focused partially coherent LG_{pl} beam with $p = 1$ and $l = 1$ obstructed by a sector shaped opaque obstacle with center angle α at several propagation distances [102]

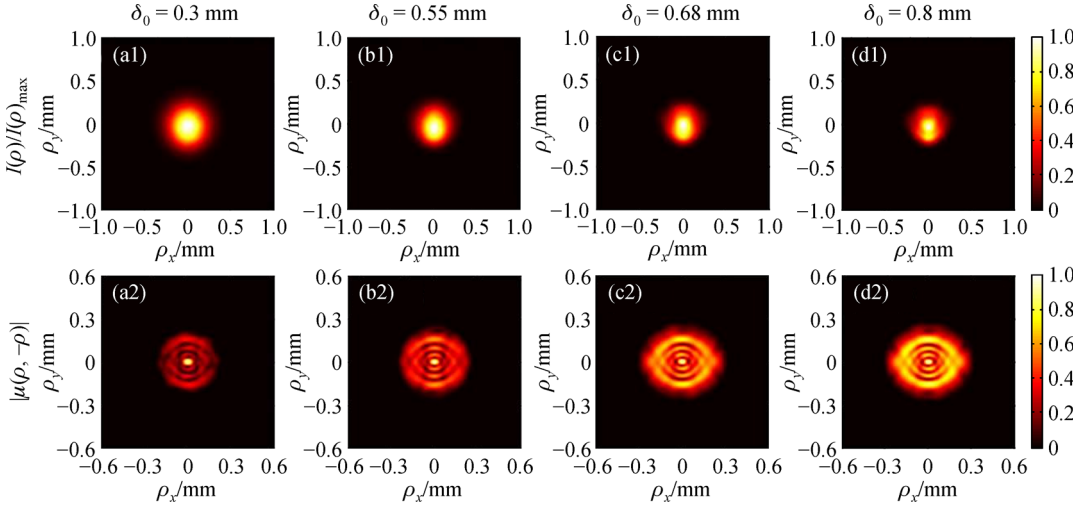

Fig. 21 Modulus of the degree of coherence of a focused partially coherent LG_{pl} beam with $p = 1$ and $l = 1$ obstructed by a sector shaped opaque obstacle with center angle $\alpha = 90°$ in the focal plane for different values of initial coherence length [102]

6 Conclusions

Recent developments on partially coherent vortex beam have been introduced both theoretically and experimentally. The basic concepts, theoretical models, generation and propagation of partially coherent vortex beams have been reviewed. Partially coherent vortex beams display some unique properties (i.e., beam shaping, beam rotation and self-reconstruction), which are useful in some applications, such as optical trapping, free-space optical communications, information encryption and decryption. From 2001 to 2017, several papers on vortex beams and partially coherent vortex beams have been published [2,48,130,142,143], and the progress of the research work in this field has been introduced systematically, we believe this field will grow further and expand rapidly, and

more and more interesting results and potential applications will be revealed.

Acknowledgements Authors are thankful for the support of the National Natural Science Foundation of China (Grant Nos. 91750201, 11525418, 11774250 and 11804198), Project of the Priority Academic Program Development of Jiangsu Higher Education Institutions.

References

1. Nye J, Berry M. Dislocations in wave trains. Proceedings of the Royal Society of London, Series A, Mathematical and Physical Sciences, 1974, 336(1605): 165–190
2. Soskin M, Vasnetsov M. Singular optics. Progress in Optics, 2001, 42(4): 219–276
3. Gbur G, Tyson R K. Vortex beam propagation through atmospheric turbulence and topological charge conservation. Journal of the Optical Society of America A, Optics, Image Science, and Vision, 2008, 25(1): 225–230
4. Zhen B, Hsu C W, Lu L, Stone A D, Soljačić M. Topological nature of optical bound states in the continuum. Physical Review Letters, 2014, 113(25): 257401
5. Flossmann F, Schwarz U, Maier M. Propagation dynamics of optical vortices in Laguerre–Gaussian beams. Optics Communications, 2005, 250(4–6): 218–230
6. Zhu K, Zhou G, Li X, Zheng X, Tang H. Propagation of Bessel-Gaussian beams with optical vortices in turbulent atmosphere. Optics Express, 2008, 16(26): 21315–21320
7. Schwarz U, Sogomonian S, Maier M. Propagation dynamics of phase dislocations embedded in a Bessel light beam. Optics Communications, 2002, 208(4–6): 255–262
8. Orlov S, Regelskis K, Smilgevičius V, Stabinis A. Propagation of Bessel beams carrying optical vortices. Optics Communications, 2002, 209(1–3): 155–165
9. Yang Y, Dong Y, Zhao C, Cai Y. Generation and propagation of an anomalous vortex beam. Optics Letters, 2013, 38(24): 5418–5421
10. Vaity P, Rusch L. Perfect vortex beam: Fourier transformation of a Bessel beam. Optics Letters, 2015, 40(4): 597–600
11. Li P, Zhang Y, Liu S, Ma C, Han L, Cheng H, Zhao J. Generation of perfect vectorial vortex beams. Optics Letters, 2016, 41(10): 2205–2208
12. Paterson C. Atmospheric turbulence and orbital angular momentum of single photons for optical communication. Physical Review Letters, 2005, 94(15): 153901
13. Thidé B, Then H, Sjöholm J, Palmer K, Bergman J, Carozzi T D, Istomin Y N, Ibragimov N H, Khamitova R. Utilization of photon orbital angular momentum in the low-frequency radio domain. Physical Review Letters, 2007, 99(8): 087701
14. Grier D G. A revolution in optical manipulation. Nature, 2003, 424 (6950): 810–816
15. O'Neil A T, Padgett M J. Axial and lateral trapping efficiency of Laguerre–Gaussian modes in inverted optical tweezers. Optics Communications, 2001, 193(1–6): 45–50
16. Ng J, Lin Z, Chan C T. Theory of optical trapping by an optical vortex beam. Physical Review Letters, 2010, 104(10): 103601
17. Wang X, Rui G, Gong L, Gu B, Cui Y. Manipulation of resonant metallic nanoparticle using 4Pi focusing system. Optics Express, 2016, 24(21): 24143–24152
18. Chen J, Wan C, Kong L J, Zhan Q. Tightly focused optical field with controllable photonic spin orientation. Optics Express, 2017, 25(16): 19517–19528
19. Molina-Terriza G, Torres J P, Torner L. Twisted photons. Nature Physics, 2007, 3(5): 305–310
20. Bozinovic N, Yue Y, Ren Y, Tur M, Kristensen P, Huang H, Willner A E, Ramachandran S. Terabit-scale orbital angular momentum mode division multiplexing in fibers. Science, 2013, 340(6140): 1545–1548
21. Vaziri A, Pan J W, Jennewein T, Weihs G, Zeilinger A. Concentration of higher dimensional entanglement: qutrits of photon orbital angular momentum. Physical Review Letters, 2003, 91(22): 227902
22. Gu Y, Gbur G. Measurement of atmospheric turbulence strength by vortex beam. Optics Communications, 2010, 283(7): 1209–1212
23. Li X, Tai Y, Zhang L, Li H, Li L. Characterization of dynamic random process using optical vortex metrology. Applied Physics B, Lasers and Optics, 2014, 116(4): 901–909
24. Tamburini F, Anzolin G, Umbriaco G, Bianchini A, Barbieri C. Overcoming the rayleigh criterion limit with optical vortices. Physical Review Letters, 2006, 97(16): 163903
25. Yu W, Ji Z, Dong D, Yang X, Xiao Y, Gong Q, Xi P, Shi K. Super-resolution deep imaging with hollow Bessel beam STED microscopy. Laser & Photonics Reviews, 2016, 10(1): 147–152
26. Beijersbergen M W, Allen L, Van der Veen H, Woerdman J. Astigmatic laser mode converters and transfer of orbital angular momentum. Optics Communications, 1993, 96(1–3): 123–132
27. Arlt J, Dholakia K. Generation of high-order Bessel beams by use of an axicon. Optics Communications, 2000, 177(1–6): 297–301
28. Beijersbergen M, Coerwinkel R, Kristensen M, Woerdman J. Helical-wavefront laser beams produced with a spiral phaseplate. Optics Communications, 1994, 112(5–6): 321–327
29. Heckenberg N R, McDuff R, Smith C P, White A G. Generation of optical phase singularities by computer-generated holograms. Optics Letters, 1992, 17(3): 221–223
30. Matsumoto N, Ando T, Inoue T, Ohtake Y, Fukuchi N, Hara T. Generation of high-quality higher-order Laguerre-Gaussian beams using liquid-crystal-on-silicon spatial light modulators. Journal of the Optical Society of America A, Optics, Image Science, and Vision, 2008, 25(7): 1642–1651
31. Marrucci L, Manzo C, Paparo D. Optical spin-to-orbital angular momentum conversion in inhomogeneous anisotropic media. Physical Review Letters, 2006, 96(16): 163905
32. Chen P, Ji W, Wei B Y, Hu W, Chigrinov V, Lu Y Q. Generation of arbitrary vector beams with liquid crystal polarization converters and vector-photoaligned q-plates. Applied Physics Letters, 2015, 107(24): 241102
33. Machavariani G, Lumer Y, Moshe I, Meir A, Jackel S. Efficient extracavity generation of radially and azimuthally polarized beams. Optics Letters, 2007, 32(11): 1468–1470
34. Naidoo D, Roux F S, Dudley A, Litvin I, Piccirillo B, Marrucci L, Forbes A. Controlled generation of higher-order Poincaré sphere

beams from a laser. Nature Photonics, 2016, 10(5): 327–332
35. Cai X, Wang J, Strain M J, Johnson-Morris B, Zhu J, Sorel M, O'Brien J L, Thompson M G, Yu S. Integrated compact optical vortex beam emitters. Science, 2012, 338(6105): 363–366
36. Fang X, Yang G, Wei D, Wei D, Ni R, Ji W, Zhang Y, Hu X, Hu W, Lu Y Q, Zhu S N, Xiao M. Coupled orbital angular momentum conversions in a quasi-periodically poled $LiTaO_3$ crystal. Optics Letters, 2016, 41(6): 1169–1172
37. Wu Y, Ni R, Xu Z, Wu Y, Fang X, Wei D, Hu X, Zhang Y, Xiao M, Zhu S. Tunable third harmonic generation of vortex beams in an optical superlattice. Optics Express, 2017, 25(25): 30820–30826
38. Leach J, Keen S, Padgett M J, Saunter C, Love G D. Direct measurement of the skew angle of the Poynting vector in a helically phased beam. Optics Express, 2006, 14(25): 11919–11924
39. Berkhout G C, Beijersbergen M W. Method for probing the orbital angular momentum of optical vortices in electromagnetic waves from astronomical objects. Physical Review Letters, 2008, 101 (10): 100801
40. Sztul H I, Alfano R R. Double-slit interference with Laguerre-Gaussian beams. Optics Letters, 2006, 31(7): 999–1001
41. Hickmann J M, Fonseca E J, Soares W C, Chávez-Cerda S. Unveiling a truncated optical lattice associated with a triangular aperture using light's orbital angular momentum. Physical Review Letters, 2010, 105(5): 053904
42. de Araujo L E, Anderson M E. Measuring vortex charge with a triangular aperture. Optics Letters, 2011, 36(6): 787–789
43. Guo C S, Yue S J, Wei G X. Measuring the orbital angular momentum of optical vortices using a multipinhole plate. Applied Physics Letters, 2009, 94(23): 231104
44. Vinu R V, Singh R K. Determining helicity and topological structure of coherent vortex beam from laser speckle. Applied Physics Letters, 2016, 109(11): 111108
45. Prabhakar S, Kumar A, Banerji J, Singh R P. Revealing the order of a vortex through its intensity record. Optics Letters, 2011, 36 (22): 4398–4400
46. Zhao P, Li S, Feng X, Cui K, Liu F, Zhang W, Huang Y. Measuring the complex orbital angular momentum spectrum of light with a mode-matching method. Optics Letters, 2017, 42(6): 1080–1083
47. Dudley A, Litvin I A, Forbes A. Quantitative measurement of the orbital angular momentum density of light. Applied Optics, 2012, 51(7): 823–833
48. Zhou H L, Fu D Z, Dong J J, Zhang P, Chen D X, Cai X L, Li F L, Zhang X L. Orbital angular momentum complex spectrum analyzer for vortex light based on the rotational Doppler effect. Light, Science & Applications, 2017, 6(4): e16251
49. Basistiy I, Soskin M, Vasnetsov M. Optical wavefront dislocations and their properties. Optics Communications, 1995, 119(5–6): 604–612
50. Lee W, Yuan X C, Dholakia K. Experimental observation of optical vortex evolution in a Gaussian beam with an embedded fractional phase step. Optics Communications, 2004, 239(1–3): 129–135
51. Berry M. Optical vortices evolving from helicoidal integer and fractional phase steps. Journal of Optics A, Pure and Applied Optics, 2004, 6(2): 259–268
52. Gbur G. Fractional vortex Hilbert's hotel. Optica, 2016, 3(3): 222–225
53. Tao S H, Lee W M, Yuan X C. Dynamic optical manipulation with a higher-order fractional bessel beam generated from a spatial light modulator. Optics Letters, 2003, 28(20): 1867–1869
54. Fang Y, Lu Q, Wang X, Zhang W, Chen L. Fractional-topological-charge-induced vortex birth and splitting of light fields on the submicron scale. Physical Review A, 2017, 95(2): 023821
55. Molchan M A, Doktorov E V, Vlasov R A. Propagation of vector fractional charge Laguerre-Gaussian light beams in the thermally nonlinear moving atmosphere. Optics Letters, 2010, 35(5): 670–672
56. Vasylkiv Y, Skab I, Vlokh R. Crossover regime of optical vortices generation via electro-optic nonlinearity: the problem of optical vortices with the fractional charge generated by crystals. Journal of the Optical Society of America A, Optics, Image Science, and Vision, 2014, 31(9): 1936–1945
57. Yang Y, Zhu X, Zeng J, Lu X, Zhao C, Cai Y. Anomalous Bessel vortex beam: modulating orbital angular momentum with propagation. Nanophotonics, 2018, 7(3): 677–682
58. Oemrawsingh S S R, de Jong J A, Ma X, Aiello A, Eliel E R, 't Hooft G W, Woerdman J P. High-dimensional mode analyzers for spatial quantum entanglement. Physical Review A, 2006, 73(3): 032339
59. Guo C S, Yu Y N, Hong Z. Optical sorting using an array of optical vortices with fractional topological charge. Optics Communications, 2010, 283(9): 1889–1893
60. Tao S, Yuan X C, Lin J, Peng X, Niu H. Fractional optical vortex beam induced rotation of particles. Optics Express, 2005, 13(20): 7726–7731
61. Situ G, Pedrini G, Osten W. Spiral phase filtering and orientation-selective edge detection/enhancement. Journal of the Optical Society of America A, Optics, Image Science, and Vision, 2009, 26(8): 1788–1797
62. Strohaber J, Boran Y, Sayrac M, Johnson L, Zhu F, Kolomenskii A, Schuessler H. Nonlinear mixing of optical vortices with fractional topological charge in Raman sideband generation. Journal of Optics, 2017, 19(1): 015607
63. Ni R, Niu Y, Du L, Hu X, Zhang Y, Zhu S. Topological charge transfer in frequency doubling of fractional orbital angular momentum state. Applied Physics Letters, 2016, 109(15): 151103
64. Born M, Wolf E. Principles of Optics: Electromagnetic Theory of Propagation, Interference and Diffraction of Light. 7nd ed. Cambridge: Cambridge University Press, 1999
65. Wolf E. New theory of partial coherence in the space–frequency domain. Part I: spectra and cross spectra of steady-state sources. Journal of the Optical Society of America, 1982, 72(3): 343–351
66. Wolf E. New theory of partial coherence in the space-frequency domain. Part II: steady-state fields and higher-order correlations. Journal of the Optical Society of America A, Optics and Image Science, 1986, 3(1): 76–85
67. Wolf E. Invariance of the spectrum of light on propagation. Physical Review Letters, 1986, 56(13): 1370–1372
68. Gori F. Collett-Wolf sources and multimode lasers. Optics Communications, 1980, 34(3): 301–305

69. Carter W H, Wolf E. Coherence and radiometry with quasihomogeneous planar sources. Journal of the Optical Society of America, 1977, 67(6): 785–796
70. Gori F. Mode propagation of the field generated by Collett-Wolf Schell-model sources. Optics Communications, 1983, 46(3–4): 149–154
71. Gori F, Guattari G, Padovani C. Modal expansion for J_0-correlated Schell-model sources. Optics Communications, 1987, 64(4): 311–316
72. Gori F, Guattari G, Palma C, Padovani C. Observation of optical redshifts and blueshifts produced by source correlations. Optics Communications, 1988, 67(1): 1–4
73. Ricklin J C, Davidson F M. Atmospheric turbulence effects on a partially coherent Gaussian beam: implications for free-space laser communication. Journal of the Optical Society of America A, Optics, Image Science, and Vision, 2002, 19(9): 1794–1802
74. Ricklin J C, Davidson F M. Atmospheric optical communication with a Gaussian Schell beam. Journal of the Optical Society of America A, Optics, Image Science, and Vision, 2003, 20(5): 856–866
75. Kato Y, Mima K, Miyanaga N, Arinaga S, Kitagawa Y, Nakatsuka M, Yamanaka C. Random phasing of high-power lasers for uniform target acceleration and plasma-instability suppression. Physical Review Letters, 1984, 53(11): 1057–1060
76. Beléndez A, Carretero L, Fimia A. The use of partially coherent light to reduce the efficiency of silver halide noise gratings. Optics Communications, 1993, 98(4–6): 236–240
77. Cai Y, Zhu S Y. Ghost imaging with incoherent and partially coherent light radiation. Physical Review E, 2005, 71(5): 056607
78. Zhao C, Cai Y, Lu X, Eyyuboğlu H T. Radiation force of coherent and partially coherent flat-topped beams on a Rayleigh particle. Optics Express, 2009, 17(3): 1753–1765
79. Zhang J F, Wang Z Y, Cheng B, Wang Q Y, Wu B, Shen X X, Zheng L L, Xu Y F, Lin Q. Atom cooling by partially spatially coherent lasers. Physical Review A., 2013, 88(2): 023416
80. Zubairy M S, McIver J K. Second-harmonic generation by a partially coherent beam. Physical Review A, 1987, 36(1): 202–206
81. Cai Y, Peschel U. Second-harmonic generation by an astigmatic partially coherent beam. Optics Express, 2007, 15(23): 15480–15492
82. van Dijk T, Fischer D G, Visser T D, Wolf E. Effects of spatial coherence on the angular distribution of radiant intensity generated by scattering on a sphere. Physical Review Letters, 2010, 104(17): 173902
83. Ding C, Cai Y, Korotkova O, Zhang Y, Pan L. Scattering-induced changes in the temporal coherence length and the pulse duration of a partially coherent plane-wave pulse. Optics Letters, 2011, 36(4): 517–519
84. Kermisch D. Partially coherent image processing by laser scanning. Journal of the Optical Society of America, 1975, 65 (8): 887–891
85. Gori F, Santarsiero M, Borghi R, Vicalvi S. Partially coherent sources with helicoidal modes. Optica Acta, 1998, 45(3): 539–554
86. Gbur G, Visser T D, Wolf E. 'Hidden' singularities in partially coherent wavefields. Journal of Optics A Pure & Applied Optics, 2004, 6(5): S239–S242
87. Visser T D, Gbur G, Wolf E. Effect of the state of coherence on the three-dimensional spectral intensity distribution near focus. Optics Communications, 2002, 213(1–3): 13–19
88. Bouchal Z, Perina J. Non-diffracting beams with controlled spatial coherence. Optica Acta, 2002, 49(10): 1673–1689
89. Gbur G, Visser T D. Coherence vortices in partially coherent beams. Optics Communications, 2003, 222(1–6): 117–125
90. Ponomarenko S A. A class of partially coherent beams carrying optical vortices. Journal of the Optical Society of America A, Optics, Image Science, and Vision, 2001, 18(1): 150–156
91. Maleev I D, Palacios D M, Marathay A S, Swartzlander G A Jr. Spatial correlation vortices in partially coherent light: theory. Journal of the Optical Society of America B, Optical Physics, 2004, 21(11): 1895–1900
92. Jeng C C, Shih M F, Motzek K, Kivshar Y. Partially incoherent optical vortices in self-focusing nonlinear media. Physical Review Letters, 2004, 92(4): 043904
93. van Dijk T, Visser T D. Evolution of singularities in a partially coherent vortex beam. Journal of the Optical Society of America. A, Optics, Image Science, and Vision, 2009, 26(4): 741–744
94. Wang F, Zhu S, Cai Y. Experimental study of the focusing properties of a Gaussian Schell-model vortex beam. Optics Letters, 2011, 36(16): 3281–3283
95. Yang Y, Chen M, Mazilu M, Mourka A, Liu Y D, Dholakia K. Effect of the radial and azimuthal mode indices of a partially coherent vortex field upon a spatial correlation singularity. New Journal of Physics, 2013, 15(11): 113053
96. Qin Z, Tao R, Zhou P, Xu X, Liu Z. Propagation of partially coherent Bessel–Gaussian beams carrying optical vortices in non-Kolmogorov turbulence. Optics & Laser Technology, 2014, 56 (33): 182–188
97. Zhang Z, Fan H, Xu H F, Qu J, Huang W. Three-dimensional focus shaping of partially coherent circularly polarized vortex beams using a binary optic. Journal of Optics, 2015, 17(6): 065611
98. Singh R K, Sharma A M, Senthilkumaran P. Vortex array embedded in a partially coherent beam. Optics Letters, 2015, 40 (12): 2751–2754
99. Liu D, Wang Y, Yin H. Evolution properties of partially coherent flat-topped vortex hollow beam in oceanic turbulence. Applied Optics, 2015, 54(35): 10510–10516
100. Cheng M, Guo L, Li J, Huang Q, Cheng Q, Zhang D. Propagation of an optical vortex carried by a partially coherent Laguerre-Gaussian beam in turbulent ocean. Applied Optics, 2016, 55(17): 4642–4648
101. Zhang Y, Ma D, Zhou Z, Yuan X. Research on partially coherent flat-topped vortex hollow beam propagation in turbulent atmosphere. Applied Optics, 2017, 56(10): 2922–2926
102. Liu X, Peng X, Liu L, Wu G, Zhao C, Wang F, Cai Y. Self-reconstruction of the degree of coherence of a partially coherent vortex beam obstructed by an opaque obstacle. Applied Physics Letters, 2017, 110(18): 181104
103. Stahl C S D, Gbur G. Partially coherent vortex beams of arbitrary order. Journal of the Optical Society of America A, Optics, Image Science, and Vision, 2017, 34(10): 1793–1799
104. Liu D, Yin H, Wang G, Wang Y. Propagation of partially coherent Lorentz-Gauss vortex beam through oceanic turbulence. Applied

Optics, 2017, 56(31): 8785–8792
105. Ostrovsky A S, García-García J, Rickenstorff-Parrao C, Olvera-Santamaría M A. Partially coherent diffraction-free vortex beams with a Bessel-mode structure. Optics Letters, 2017, 42(24): 5182–5185
106. Gori F, Santarsiero M. Devising genuine spatial correlation functions. Optics Letters, 2007, 32(24): 3531–3533
107. Gori F, Ramirezsanchez V, Santarsiero M, Shirai T. On genuine cross-spectral density matrices. Journal of Optics A, 2009, 11(8): 085706
108. Chen Y, Liu L, Wang F, Zhao C, Cai Y. Elliptical Laguerre-Gaussian correlated Schell-model beam. Optics Express, 2014, 22 (11): 13975–13987
109. Tong Z, Korotkova O. Electromagnetic nonuniformly correlated beams. Journal of the Optical Society of America A, Optics, Image Science, and Vision, 2012, 29(10): 2154–2158
110. Lajunen H, Saastamoinen T. Non-uniformly correlated partially coherent pulses. Optics Express, 2013, 21(1): 190–195
111. Sahin S, Korotkova O. Light sources generating far fields with tunable flat profiles. Optics Letters, 2012, 37(14): 2970–2972
112. Zhang Y, Liu L, Zhao C, Cai Y. Multi-Gaussian Schell-model vortex beam. Physics Letters A, 2014, 378(9): 750–754
113. Chen Y, Wang F, Zhao C, Cai Y. Experimental demonstration of a Laguerre-Gaussian correlated Schell-model vortex beam. Optics Express, 2014, 22(5): 5826–5838
114. Liu H, Chen D, Xia J, Lü Y, Zhang L, Pu X. Influences of uniaxial crystal on partially coherent multi-Gaussian Schell-model vortex beams. Optical Engineering (Redondo Beach, Calif.), 2016, 55 (11): 116101
115. Liu X, Wang F, Liu L, Zhao C, Cai Y. Generation and propagation of an electromagnetic Gaussian Schell-model vortex beam. Journal of the Optical Society of America A, Optics, Image Science, and Vision, 2015, 32(11): 2058–2065
116. Zhang Y, Pan L, Cai Y. Propagation of Correlation Singularities of a Partially Coherent Laguerre-Gaussian Electromagnetic Beam in a Uniaxial Crystal. IEEE Photonics Journal, 2017, 9(4): 1–13
117. Guo L, Chen Y, Liu X, Liu L, Cai Y. Vortex phase-induced changes of the statistical properties of a partially coherent radially polarized beam. Optics Express, 2016, 24(13): 13714–13728
118. Zhao C, Cai Y. Trapping two types of particles using a focused partially coherent elegant Laguerre-Gaussian beam. Optics Letters, 2011, 36(12): 2251–2253
119. Liu X, Shen Y, Liu L, Wang F, Cai Y. Experimental demonstration of vortex phase-induced reduction in scintillation of a partially coherent beam. Optics Letters, 2013, 38(24): 5323–5326
120. Zeng J, Liu X, Wang F, Zhao C, Cai Y. Partially coherent fractional vortex beam. Optics Express, 2018, 26(21): 26830–26844
121. Perez-Garcia B, Yepiz A, Hernandez-Aranda R I, Forbes A, Swartzlander G A. Digital generation of partially coherent vortex beams. Optics Letters, 2016, 41(15): 3471–3474
122. Liu R, Wang F, Chen D, Wang Y, Zhou Y, Gao H, Zhang P, Li F. Measuring mode indices of a partially coherent vortex beam with Hanbury Brown and Twiss type experiment. Applied Physics Letters, 2016, 108(5): 051107
123. Pires H D, Woudenberg J, van Exter M P. Measurements of spatial coherence of partially coherent light with and without orbital angular momentum. Journal of the Optical Society of America A, Optics, Image Science, and Vision, 2010, 27(12): 2630–2637
124. Pires H D, Woudenberg J, van Exter M P. Measurement of the orbital angular momentum spectrum of partially coherent beams. Optics Letters, 2010, 35(6): 889–891
125. Zhao C, Wang F, Dong Y, Han Y, Cai Y. Effect of spatial coherence on determining the topological charge of a vortex beam. Applied Physics Letters, 2012, 101(26): 261104
126. Yang Y, Mazilu M, Dholakia K. Measuring the orbital angular momentum of partially coherent optical vortices through singularities in their cross-spectral density functions. Optics Letters, 2012, 37(23): 4949–4951
127. Escalante A Y, Perezgarcia B, Hernandezaranda R I, Swartzlander G A. Determination of angular momentum content in partially coherent beams through cross correlation measurements. In: Proceedings of SPIE Laser Beam Shaping. SPIE, 2013, 884302
128. Kotlyar V V, Almazov A A, Khonina S N, Soifer V A, Elfstrom H, Turunen J. Generation of phase singularity through diffracting a plane or Gaussian beam by a spiral phase plate. Journal of the Optical Society of America A, Optics, Image Science, and Vision, 2005, 22(5): 849–861
129. Wang F, Cai Y, Korotkova O. Partially coherent standard and elegant Laguerre-Gaussian beams of all orders. Optics Express, 2009, 17(25): 22366–22379
130. Dennis M R, O'Holleran K, Padgett M J. Chapter 5 Singular Optics: Optical Vortices and Polarization Singularities. Progress in Optics, 2009, 53: 293–363
131. Bogatyryova G V, Fel'de C V, Polyanskii P V, Ponomarenko S A, Soskin M S, Wolf E. Partially coherent vortex beams with a separable phase. Optics Letters, 2003, 28(11): 878–880
132. Mandel L, Wolf E. Optical Coherence and Quantum Optics. Cambridge: Cambridge University Press, 2001, 1–1194
133. Palacios D M, Maleev I D, Marathay A S, Swartzlander G A Jr. Spatial correlation singularity of a vortex field. Physical Review Letters, 2004, 92(14): 143905
134. Wolf E. Introduction to the Theory of Coherence and Polarization of Light. Cambridge: Cambridge University Press, 2007
135. Cai Y, Chen Y, Wang F. Generation and propagation of partially coherent beams with nonconventional correlation functions: a review. Journal of the Optical Society of America A, Optics, Image Science, and Vision, 2014, 31(9): 2083–2096
136. Ren Y X, Lu R D, Gong L. Tailoring light with a digital micromirror device. Annalen der Physik, 2015, 527(7–8): 447–470
137. De Santis P, Gori F, Guattari G, Palma C. An example of a Collett-Wolf source. Optics Communications, 1979, 29(3): 256–260
138. Ostrovsky A S, García E H. Modulation of spatial coherence of optical field by means of liquid crystal light modulator. Revista Mexicana de Física, 2005, 51(5): 442–446
139. Liu X, Wu T, Liu L, Zhao C, Cai Y. Experimental determination of the azimuthal and radial mode orders of a partially coherent LG_{pl} beam. Chinese Optics Letters, 2017, 15(3): 030002–030006
140. Wang F, Liu X, Yuan Y, Cai Y. Experimental generation of partially coherent beams with different complex degrees of coherence. Optics Letters, 2013, 38(11): 1814–1816
141. Chen J, Liu X, Yu J, Cai Y. Simultaneous determination of the sign and the magnitude of the topological charge of a partially coherent

vortex beam. Applied Physics B, Lasers and Optics, 2016, 122(7): 201

142. Polyanskii P V. Some current views on singular optics. In: Proceedings of SPIE 6th International Conference on Correlation Optics. SPIE, 2004, 31–41
143. Soskin M, Boriskina S V, Chong Y, Dennis M R, Desyatnikov A. Singular optics and topological photonics. Journal of Optics, 2017, 19(1): 010401

Jun Zeng spent his bachelor time at Hubei University of Arts and Science (Xiangyang, China). He studied at Taiyuan University of Science and Technology (Taiyuan, China) for his Master's degree in optics from 2013 to 2016. Since September 2017, he became a Ph.D. candidate in School of Physical Science and Technology at Soochow University (Suzhou, China). His research topics include singular optics, atmospheric optics and optical measurement.

Rong Lin spent her bachelor time at Heze University (Heze, China). she received her master's degree in 2012 from Shandong Normal University (Jinan, China) in 2009. Since September 2012, she became a teacher in College of Physics and Electronic Engineering, Heze University. Since September 2018, she became a Ph.D. candidate in School of Physics and Electronics, Shandong Normal University. Her research topics include optical coherence and nonlinear optics.

Xianlong Liu spent his bachelor time at Yanbian University (Jilin), and got his master's degree at Soochow University (Jiangsu) in 2013. Latter he became a Ph.D. candidate in School of Physical Science and Technology, Soochow University, and got his doctor's degree at 2017. He spent a year in Netherland as a Joint Ph.D. student at VU University of Amsterdam in 2017. His research topic includes laser optics, atmospheric optics and optical imaging.

Chengliang Zhao is a professor of School of Physical Science and Technology, Soochow University, China. He received his Ph.D. degree in Physics from Zhejiang University. His research interests include coherent optics, diffractive imaging, phase retrieval and optical tweezers.

Yangjian Cai is a professor of School of Physical Science and Technology, Soochow University, and also a professor of School of Physics and Electronics, Shandong Normal University, China. He received his B.Sc. degree in Physics at Zhejiang University, Ph.D. degree in Physics at Zhejiang University and Ph.D. degree in Electromagnetic theory at Royal Institute of Technology. In 2015, he obtained the National Science Fund for Distinguished Young Scholars. His research interests include optical coherence and polarization, propagation, optical imaging, particle trapping, turbulent atmosphere. He has published over 300 papers in refereed international journals, and he is a topical editor of *JOSA A*, a topical editor of *PhotoniX* and an editorial board member of *Progress in Optics*.